Quantification of Triple Single-Leg Hop Test Kinematic Parameters using Inertial Sensors: A Validated Method for Functional Assessments after Knee Injury

by

Niloufar Ahmadian

A thesis submitted in partial fulfillment of the requirements for the degree of

Master of Science

Department of Mechanical Engineering
University of Alberta

Abstract

Severe knee injuries such as anterior cruciate ligament (ACL) and meniscus tears, can have a serious effect on the lives of young athletes. Consequences may include an inability to return to previous levels of activity, an increased risk of re-injury or contralateral injury upon return to sport (RTS), and early-onset osteoarthritis. Horizontal hop tests are commonly used to monitor functional performance after a youth sport-related knee injury and assess it prior to RTS. Traditionally, the symmetry of total distance hopped, or time to hop a set distance, between injured and uninjured limbs is expressed as a limb symmetry index (LSI). However, clinical decisions based upon LSIs may be misleading, as kinematic and kinetic deficiencies of lower limbs may exist independent of symmetrical hop performance.

Despite providing robust data about kinematic features of movement, motion-capture systems used for research-based purposes are not compatible with typical clinical environments given that they are expensive, and require specialized operators and lengthy data post-processing. Therefore, an alternative measurement system that can reveal robust in-depth kinematic details of functional tests, including hopping tests, is required in clinical research settings.

This research aimed to: (1) develop a methodology for kinematic measurements during horizontal hop tests using a wearable system of inertial measurement units (IMUs), (2) validate the accuracy and precision of the estimated knee and ankle angles, initial and terminal contact instants, and foot forward progression along the hops against a reference motion-capture system, and (3) evaluate the applicability of this system in a clinical research environment during triple single leg hop (TSLH) test to highlight kinematic differences between injured and uninjured leg groups during hopping, with clinically relevant outcome measures.

First, a system of 3 IMUs was applied on the dominant leg of 10 able-bodied participants while each performed two TSLH trials. Foot-ground initial contact (IC) and terminal contact (TC) instants were calculated based on kinematic features of foot and shank-mounted accelerometers and gyroscopes recordings. 3D knee and ankle angles were calculated using the strap-down integration method. Further, anterior foot trajectory during the TSLH was calculated by double integration of gravity-free foot acceleration and implementation of velocity correction techniques. The errors of these estimated quantities were calculated in comparison to the joint angles and temporospatial parameters obtained with a motion-capture system. Secondly, a system of 3 IMUs per limb was applied to 22 youth with a sport-related unilateral intra-articular knee injury and 10 uninjured youth while each performed two trials of TSLH bilaterally. All estimated kinematic parameters (except for coronal and transverse joint angles) were compared side-to-side and between the leg groups of injured and uninjured individuals, using Wilcoxon signed-rank test and Wilcoxon rank-sum test, respectively. Additionally, Spearman's correlation was assessed between temporospatial parameters and all subscales of Knee Injury and Osteoarthritis Outcome Score (KOOS) within the injured group. Finally, the LSIs of kinematic parameters were compared between injured and uninjured groups, using Wilcoxon rank-sum test (α=0.05).

Overall (for all the 10 able-bodied participants, all hop phases, all anatomical planes), root-mean-square (RMS), and range of motion (ROM) error medians were below 2.3 and 3.2 degrees for knee and ankle angles, and correlation coefficient medians of IMU-based and camera-based joint angles exceeded 0.92 for both joints. IC and TC instants were estimated with median errors less than 2 ms and 11 ms, respectively, while individual hop distances and total TSLH progression were estimated with median relative errors less than 4.5% and 2.5% of camera-based recordings. During the third flying phase, knee sagittal ROM (flexion/extension) was significantly smaller

(p=0.009) for the injured side of the injured group, compared to the uninjured group. Additionally, the knee ROM symmetry indices were significantly smaller (p=0.017) for the injured group compared to the uninjured group. Concurrently, injured participants demonstrated significant side-to-side differences (p=0.008) on ankle ROM (dorsiflexion/plantarflexion), with the uninjured side showing greater ROM. Furthermore, all hop distances and the second flying time of TSLH were moderate- to strongly correlated with KOOS Symptom and Function in Daily Living (ADL) scores (r>0.4 except for the third hop distance).

In conclusion, a novel method of detailed kinematic monitoring in clinical research environments was introduced for horizontal hop tests based on a wearable system of IMUs. This system has the appropriate accuracy and precision to reveal kinematic differences between hopping strategies adopted by injured limbs with acute knee injuries and uninjured limbs.

Preface

This thesis is an original work by Niloufar Ahmadian. The research projects that are partly covered in this thesis have received approval from the Health Research Ethics Board of University of Alberta, under project names, “Accuracy Assessment of Wearable Technologies for Objective Clinical Outcome Evaluation” and “Modifiable Factors that Compound Risk for Osteoarthritis” and study ID numbers Pro00065804 and Pro00063773, respectively.

Chapter 3 of this thesis has been submitted as an original article (research paper) to the *Clinical Biomechanics* journal and titled as: **“Instrumented Triple Single-Leg Hop Test: A Validated Method for Ambulatory Measurement of Ankle and Knee Angles using Inertial Sensors”**.

Chapter 4 of this thesis has been submitted as an original article (research paper) to *Journal of Biomechanical Engineering* and titled as: **“Quantification of Triple Single-Leg Hop Test Temporospatial Parameters: A Validated Method using Body-Worn Sensors for Functionality Evaluations after Knee Injury”**.

Chapters 3 and 4 of this thesis present a methodology development, data analyses, and interpretation of the collected experimental data that are the original contribution of Niloufar Ahmadian. The experimental data of Technical Validation study (ID: Pro00065804) were collected by Mr. Milad Nazarahari at the research facility of the Glenrose Rehabilitation Hospital. The experimental data of Clinical Research Application study (ID: Pro00063773) were collected by Niloufar Ahmadian at the research laboratory of Dr. Jackie Whittaker in Corbett Hall.

For the Technical Validation study, the experimental protocol and the application for ethics approval were written by Dr. Hossein Rouhani. For the Clinical Research Application study, the experimental protocol and the application for ethics approval were originally written by Dr. Jackie Whittaker, and Niloufar Ahmadian helped with the writing of an amendment to the latter and incorporation of inertial sensors in the experimental protocol, under supervision of Dr. Rouhani.

Research studies regarding gait temporal parameters detection, which were inspired by the methodology developed in this thesis were presented as a poster at *Spotlight on Innovation: Health to Home (2018)* (Hosted by the Glenrose Rehabilitation Hospital, Edmonton, Canada) and as a

conference presentation at the joint congress of the Canadian Society for Mechanical Engineering and CFD Society of Canada (*CSME – CFDCS Congress 2019,* London, Canada).

Dedicated to my dearest ones

who have given me life at every breath:

My Loving Mom,

My Devoted Dad,

My Darling Sister, Nasim

And

To the Beautiful Soul of Maestro James Horner!

In loving memory of

My fantastic professor, Dr. Pedram Mousavi

My dear friend, Nasim Rahmanifar

And all the beautiful lives lost in the flight PS752.

Acknowledgments

I would like to express my deep and sincere gratitude to my supervisors, Dr. Hossein Rouhani and Dr. Jackie Whittaker, who have immensely helped me with their extraordinary knowledge and expertise, incredible guidance, generous support, and kind patience during all the stages of this project. I will be forever grateful for both the scientific and life lessons that they have taught me to become a better person and reach my professional goals and dreams. I also would like to deeply thank Dr. Morris Flynn and Dr. Albert Vette, who have always supported me like dedicated supervisors, followed my academic progress, and made me hopeful about a bright future.

I would like to sincerely thank my dear friend Milad Nazarahari, for all his guidance, motivation, support, and friendship. Whenever I faced a problem during working on this project, he has offered me the best of his fantastic knowledge, and whenever I needed any consultation about my life or future goals, he has given me the best advice. Special and huge thanks also go to Alireza Noamani for always helping me whenever I needed his assistance and generously offering his time to teach me the concepts of human movement analysis.

I would like to thank my friends and lab-mates: Nasim Rahmanifar, Karla Martínez, Samira Doostie, Hosein Bahari, Ramin Fathian, Aminreza Khandan, Fatameh Gholibeigian, Sanjot Sunner, as well as Dr. Whittaker's students and collaborators, Christina Le, Linda Truong, Christopher Holt, Joshua Kennedy, and Miki Nguyen for kindly helping me with the experiments or supporting me in my daily challenges. Many thanks also go to Mr. Justin Lewicke, who has helped us with motion-capture data collection and taught me the basics of marker reconstruction.

Lastly but most importantly, I would like to thank my dearest ones with all my heart: my brilliant mom, Farkhondeh Sayedi, who has dedicated every moment of her life to her children; my fabulous dad, Majid Ahmadian, who has opened the doors of opportunities for me; my lovely kind sister, Nasim Ahmadian, who has always been my source of support and love, my caring fantastic friends all over the world who accompany and support me every day to reach my goals and dreams; and the brilliant maestro James Horner, who has been my soul healer, and has always brought tranquility and motivation into my life, with his heavenly unparalleled music. I cannot imagine how I could live without the immense love and heartfelt support of these wonderful people at every moment of my life, and especially during this project.

Table of Contents

List of Tables

List of Figures

Nomenclature

2D	2-Dimensional
3D	3-Dimensional
ACL	Anterior Cruciate Ligament
ADL	Function in Daily Living
B	Both Sides
BAF	Bony Anatomical Frame
D	Dominant Side
G_I	Injured Group
G_{UI}	Uninjured Group
I	Injured Side
IC	Initial (Foot-Ground) Contact
IKDC	International Knee Documentation Committee
IMU	Inertial Measurement Unit
IQR	Inter-Quartile Range
ISB	International Society of Biomechanics
KOOS	Knee Injury and Osteoarthritis Outcome Score
L	Left
LF	Lab Frame
LSI	Limb Symmetry Index
M	Man
n	Number of Participants
ND	Non-Dominant Side
NI	Non-Injured Side
QoL	Quality of Life
R	Right
Ref.	Reference Value
RMS	Root-Mean-Square
ROM	Range of Motion
RTS	Return to Sport
Sport/Rec	Function in Sports and Recreation
TC	Terminal (Foot-Ground) Contact
TF	Technical Frame
TSLH	Triple Single-Leg Hop
W	Woman

Chapter 1

1 Introduction

Sport-related injuries compose 35% of all types of injury in Canada and are the most prevalent cause of injury in youth [1,2]. Approximately 66% of injuries among adolescents in Canada with 12-19 years of age happen during sport [1]. Studies from Scandinavia also show a tremendous rate of sport-related injuries, accounting for 10-19% of the injuries that need emergency room treatments [3]. Accounting for over 40% of sport-related injuries among youth [2,3], knee and ankle are the most common sites exposed to the risk of injury. Severe knee injuries such as an Anterior cruciate ligament (ACL) tear have been reported to impose considerable burden over the life of approximately 250,000 Americans each year, of which 50% are 15-25 years old [4]. This population mostly includes active individuals who participate in pivoting sports such as soccer, floorball, basketball, handball, and downhill skiing [3,5].

The life of individuals and particularly athletes who sustain severe knee injuries is not only influenced by time lost from sport and treatment costs, but also with serious short- and long-term difficulties such as high risk of contralateral/re-injury after return to sport (RTS), decreased level of activity, and early-onset osteoarthritis development [3,6,7]. The risk of post-traumatic osteoarthritis development has been reported to increase by 10-fold within 12-20 years after severe knee injuries [2,8]. From every two individuals with ACL or meniscus injury, one will eventually develop knee osteoarthritis [2,3]. Additionally, the results of meta-analyses conducted in 2010 show that only about 65% of athletes return to their pre-injury level of activity after ACL reconstruction [9,10]. Among these, 3-22% re-tear the ligaments of the reconstructed knee, and 3-24% experience ACL tear on their contralateral side within the first two years of RTS [10]. Among the athletes with ACL reconstruction who do not return to sport, half of them report their ACL injury as the main reason for being less active [10]. These consequences of severe knee injuries together with evidence of the reduced rate of re-injury after gaining better functional performance and quadriceps strength necessitate the evaluation of functional performance before the athletes return to sport [10,11].

Field-based and functional tests such as single-leg hop, triple single-leg hop (TSLH), triple crossover hop, 6-m timed hop, vertical jumping, star excursion balance, and unipedal balance tests have been widely assessed to study the relationship between functional performance and power, strength, balance, passive joint laxity, and knee stability following knee joint injuries [6,7,12–14]. These functional assessments can be done without complicated equipment, time-consuming calibration and set-up processes, and with little training of the personnel while giving insightful knowledge regarding asymmetries in the functional performance of injured and uninjured sides. Therefore, these tests are commonly used for assessment of sport-related injuries and athletic performances, as well as progress evaluation in rehabilitation programs before RTS [6,12,13].

During assessments, performance of the injured limb is compared to the uninjured limb typically in terms of limb symmetry index (LSI), which is the most common reported criterion of functional assessments with horizontal hop tests [7,15]. As higher LSIs were shown to be associated with the rates of successful RTS and reduced re-injury, thresholds ranging from 80% to 90% have been considered for the LSI values by the literature before clearance for RTS [15]. In 2011, the European Board of Sports Rehabilitation published the criteria that should be considered to decide about the physical readiness of patients for RTS. According to these criteria, patients that show full knee flexor and extensor strength, and have LSI scores higher than 90% during the hop tests are considered ready for RTS [4,11]. However, recent investigations have shown that kinematic and kinetic deficiencies of the lower limbs may remain persistent even after RTS and symmetrical restoration of muscular strength [16,17].

Lower limb functional tests have been mainly analyzed with four different methods, including: (1) self-assessment, (2) visual analysis conducted by a physiotherapist, (3) depth camera-based system, and (4) motion-capture system [18]. Due to the inaccuracy, limitations, and biases involved in the first three methods, motion-capture cameras have been widely used by researchers in dedicated laboratories to study the kinematics of horizontal hop tests and the post-injury mechanisms adopted by lower limb [16,18–21]. However, such systems are costly and time-intensive for calibration, set-up, and data post-processing, require trained operators, and are not always available in clinical or all research environments for knee injury assessments [18,22]. Therefore, there is an immediate need for a relatively inexpensive measurement system with

minimal calibration time, data post-processing, and required expertise, which is compatible with ease of conducting short functional tests with minimal equipment.

Inertial measurement units (IMUs), which are composed of 3D accelerometer and 3D gyroscope, have been widely used for temporospatial and joint angles analyses of gait [23–29]. Recently, IMUs have been utilized to monitor the kinematics of vertical jumping [30–34], with promising outcomes. Therefore, although IMUs have never been used for kinematic assessment during horizontal hop tests, we hypothesize that they can be appropriate tools for detailed monitoring of horizontal hop tests to examine the injury effects on the kinematics of hopping.

Thus, the goals of this research were to: (1) develop algorithms for accurate, precise, and objective measurement of 3D knee and ankle joint angles and temporospatial parameters (i.e., foot forward progression and flying/landing times) of hopping during the TSLH functional test, using a wearable system of IMUs, and (2) Evaluate the applicability and efficacy of this system in a clinical research setting to highlight differences in kinematics of hopping between injured and uninjured leg groups, with clinically relevant measures.

1.1 Specific Aims

In order to reach the aforementioned goals, the specific aims of this research were defined as follows:

1. Estimation of 3D knee and ankle angles based on the strap-down integration of gyroscope readouts, according to the definition of the joint coordinate system during all phases of the TSLH,
2. Identification of kinematic signal features of foot- and shank-mounted IMUs for detection of foot-ground initial and terminal contact instants of each hop to split TSLH test into flying/landing phases,
3. Estimation of foot frontal progression during TSLH test to obtain the total and individual hop distances (referred to each of the three hops, performed during the TSLH test), based on foot frontal acceleration and defining a corrective function to remove the integration drifts,
4. Validation of the estimated IMU-based 3D joint angles and temporospatial parameters of TSLH test against a reference system of motion-capture cameras for 10 able-bodied participants and improvement of the algorithms to obtain accuracy (medians of errors) and precision (inter-quartile ranges of errors) comparable with similar gait studies,

5. Application of the IMU-based wearable system on two groups of participants, including 22 youth with sport-related unilateral knee injuries and 10 uninjured youth in a clinical research setting and comparison of their side-to-side and between-groups differences in hopping kinematics,

6. Calculation of LSIs for injured and uninjured youth based on estimated sagittal joint angles, flying/landing times, and individual and total hop distances and comparison of the LSI values between the injured and uninjured groups,

7. Comparison of IMU-based TSLH total distance and LSI for injured and uninjured youth with the results obtained with a measuring tape, typically used in clinical settings,

8. Calculation of the correlation coefficients between the estimated TSLH temporospatial parameters and self-reported KOOS scores of the injured participants to ensure the clinical relevance of the estimated parameters.

1.2 Thesis Outline

Chapter two reviews the relevant clinical and technical literature to this thesis and includes: a description of functional tests and horizontal hop tests, a description of a clinical questionnaire for self-assessment of knee injuries, an overview of biomechanical research that has been conducted to assess kinematics of the lower limbs during horizontal hop tests for injured and uninjured groups, an overview of the popular stationary and ambulatory systems for measurements of human locomotion kinematics, an overview of the methods implemented in the research literature to obtain joint angles, temporal parameters, and spatial parameters of human locomotion with IMUs, and an overview of the research literature that has used a system of IMUs for monitoring the kinematics of vertical jumping functional tests. Chapter 3 presents a method for estimating 3D knee and ankle joint angles with IMUs during TSLH test, shows the accuracy and precision of the estimated angles against a reference motion-capture system, and presents the results of comparing IMU-based sagittal joints range of motion (ROM) between injured and uninjured participants in a clinical research setting. Chapter 4 presents a method for estimating temporospatial parameters of the TSLH test with IMUs, shows the accuracy and precision of the estimated temporospatial parameters against a reference motion-capture system, and presents the results of comparing the IMU-based temporospatial parameters between injured and uninjured participants as well as analysis of the relevance between these parameters and patient-reported scores for symptom and function. Chapter 5 summarizes the key findings and contributions of this thesis, reviews the

complexities of using IMUs for kinematic measurements during the TSLH test compared to gait, discusses the efficacy of the applied method compared to the methods implemented in vertical jumping studies, and provides remarks on future perspectives and further research opportunities in this field. Fig. 1 illustrates an overview of the accomplished steps in this thesis project.

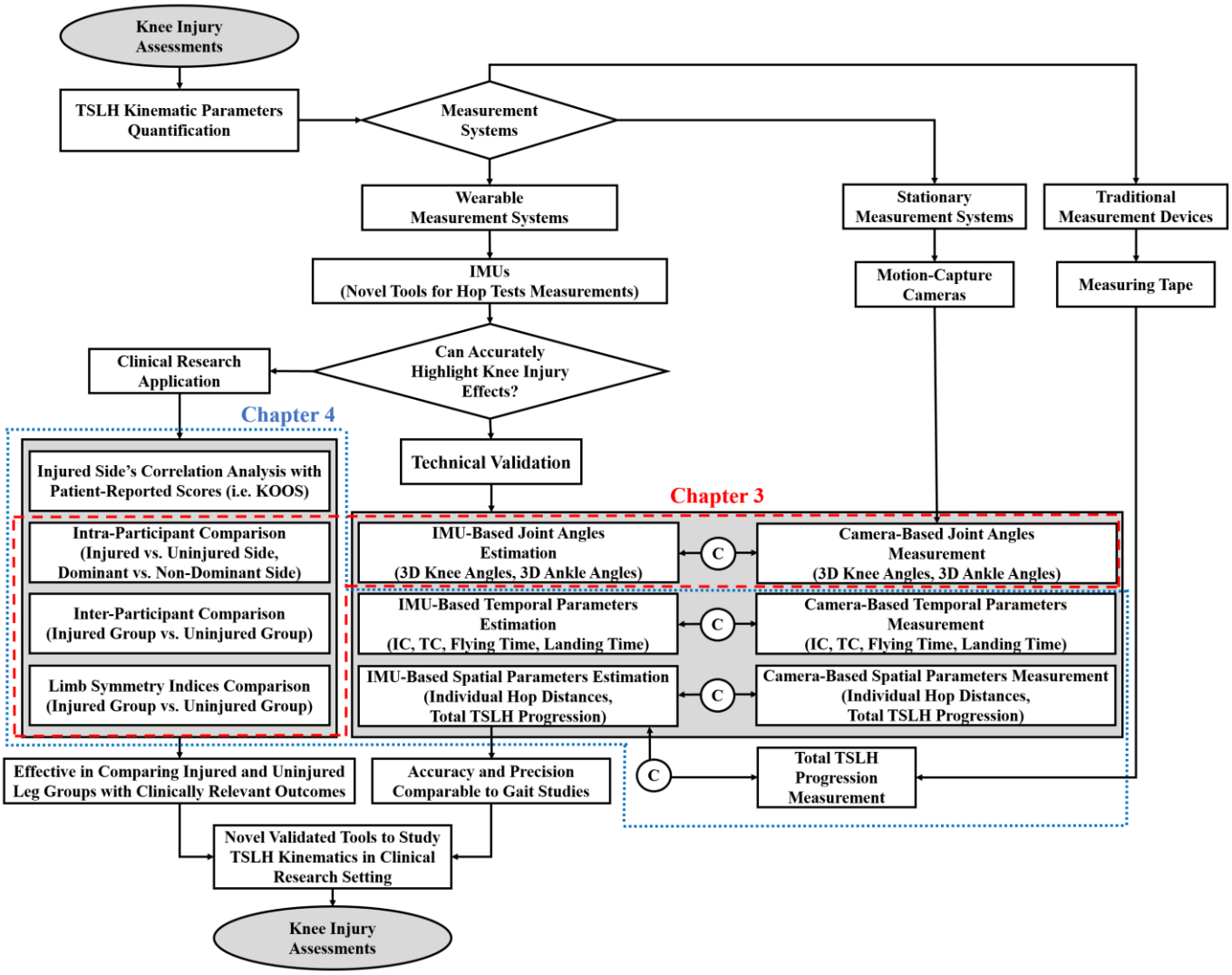

Fig. 1. Thesis outline and an overview of the accomplished steps for the quantification of TSLH kinematic parameters in the clinical research environment, using IMUs. The "C" letters within circles stand for the "Comparison" between the rectangles, which are connected with arrows. IC and TC refer to the foot-ground initial contact and terminal contact instants, respectively.

Chapter 2

2 Literature Review

2.1 Functional Tests

Functional tests are activities that are developed to objectively assess the functional limitations in simulated activity conditions, and therefore, can evaluate the progress to a higher level of functionality [16,35]. These tests can provide relevant measures for examining deficits between extremities after severe knee injuries [33]. Functional tests are regularly used in clinical settings and can be performed quickly, without the use of complicated instrumentation and advanced training of the personnel [16,36]. Two major types of the most common functional tests performed in clinical settings to assess lower limb function are horizontal hop tests and vertical jumping tests.

2.1.1 Horizontal Hop Tests

Horizontal hop tests are commonly used after ACL injuries, surgical reconstruction, and during knee rehabilitation programs to measure functional performance, assess knee stability and lower extremity muscular strength, evaluate the progress during knee rehabilitation, and determine the effect of surgical interventions [13,37]. These tests are highly demanding activities, which require a considerable amount of knee joint moment and power during the takeoff [37]. The horizontal hop tests that are commonly used in clinics and have received more attention in the literature include single-leg hop, triple single-leg hop, triple crossover hop, and 6-m timed hop tests [16,36,38]. The first three of these tests are performed with the goal of attaining maximal hop distance while in the last one, the goal is to perform the test in the shortest amount of time. Fig. 2 shows the schematic of the performance of horizontal hop tests.

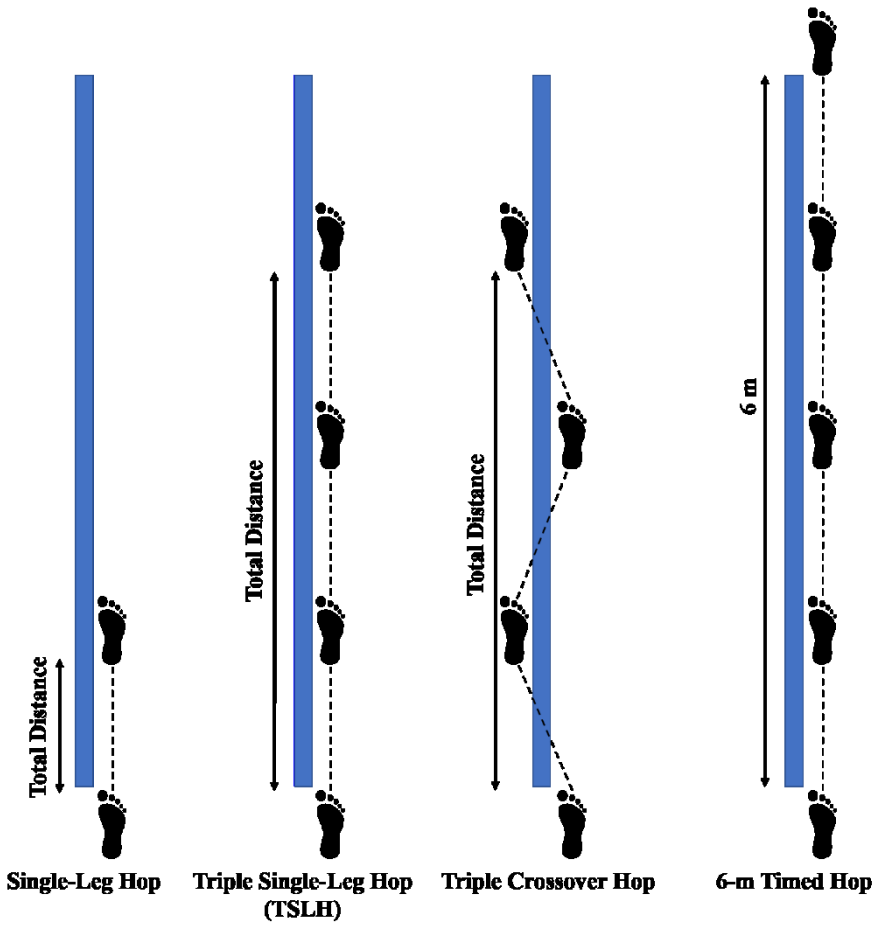

Fig. 2. The schematic of the most common horizontal hop tests, performed in clinics and for research purposes

The most common reported criterion to quantify the functional performance with hop tests is limb symmetry index (LSI), which is expressed as a percentage and can be calculated according to Eq. (1) and Eq. (2) for distance-based and time-based tests, respectively [7,37,39].

$$LSI = \frac{d_{involved}}{d_{uninvolved}} \times 100 \tag{1}$$

$$LSI = \frac{t_{uninvolved}}{t_{involved}} \times 100 \tag{2}$$

In Eqs. (1) and (2), $d_{involved}$ and $d_{uninvolved}$ denote the hopped distance on the involved (injured) limb and uninvolved (uninjured) limb, respectively; and $t_{uninvolved}$ and $t_{involved}$ denote the time required to accomplish the hop task on the uninvolved and involved limb, respectively.

Previous studies have reported that LSIs of 85% or higher for distance reached during hop tests would fall within the normal functional range [35,39], while LSIs of above 90% are recommended for a safer return to sport-specific activities [16]. However, LSIs are affected by the development of compensatory mechanisms by the adjacent joints to maintain the symmetrical performance of both limbs, and/or deficiencies of the contralateral leg following an injury or surgery [19,20,40]. Therefore, assuming guaranteed symmetrical or unimpaired biomechanics of hopping for both limbs when LSI values are higher than the aforementioned thresholds, could be misleading [20,40].

The functional hop tests for distance have been reported to provide valid and reliable measurements, with an intraclass correlation coefficient range of 0.92 to 0.96 [7,16,35]. However, in a systematic review of functional tests and their measurement properties, Hegedus et al. [41] acknowledged the contradictory results and poor methodology of the studies that have assessed reliability, criterion validity, construct validity, and responsiveness of functional tests. Therefore, the authors concluded that clinical decision making should be done cautiously based on the results of these tests [41].

2.1.1.1 Triple Single-Leg Hop (TSLH) Test

Triple single-leg hop test is a horizontal hop test in which the participant is required to perform three consecutive hops with maximal distance, and without pauses in between, and maintain their balance after the last landing, without using the contralateral leg (Fig. 3). Commonly, a measuring tape is fixed on the floor for the participants to line their toes behind the zero mark, and the test is first performed on the uninvolved limb. The total hop distance is recorded after the third hop, from the zero mark up to the heel of the testing leg [12,36].

The primary deviations of studies' protocols for performing TSLH test are: (1) whether the participants are allowed to use their arms for generating momentum during the hops, (2) whether the test is performed bare feet or with shoes, (3) how the dominant leg of the participant is identified, and (4) if the average hop distance among the trials is considered for the analyses and clinical decision making, or the longest distance hopped.

Fig. 3. The schematic of the TSLH test (A measuring tape is typically secured on the ground to measure the total hop distance but is not shown in this figure). This picture is adopted from www.simplygym.net and accessed on July 27th, 2019.

2.2 Knee Injury and Osteoarthritis Outcome Score (KOOS)

To assess patients' symptoms and function after knee ligaments and meniscus injury, the patient-administered Knee Injury and Osteoarthritis Outcome Score (KOOS) questionnaire was developed in the 1990s [42]. The KOOS has been used to measure the effectiveness of clinical interventions (e.g., surgical, rehabilitative, and pharmacological interventions) following a knee injury or osteoarthritis and to monitor the course of disease in young, middle-aged and elderly individuals [42,43]. As a patient-administered outcome measure, KOOS eliminates the observer bias, which is the deficiency of non-self-reported clinical outcome measures, obtained by the surgeons and/or their assistants [42].

The five subscales of KOOS are: Symptoms (7 items), Pain (9 items), Function in Daily Living (also called ADL, 17 items), Function in Sports and Recreation (Also called Sport/Rec, 5 items), and Knee-Related Quality of Life (also called QoL, 4 items). Accordingly, KOOS includes 42 Likert-scale questions in total (See Appendix A) that can be scored 0 (indicating no problem) to 4 (indicating extreme problems). The raw scores of each subscale are then averaged separately and converted to a 0-100 scale, according to Eq. (3), to adapt with common orthopedic scores in which zero indicates extreme knee problems, and 100 indicates no knee problem [42,44]. Calculating an

aggregate KOOS score is not recommended as the outcome of each subscale is supposed to be analyzed and interpreted distinctly [42].

$$KOOS_{Subscale} = 100 - \frac{Mean\ raw\ score\ of\ subscale\ \times 100}{4} \quad (3)$$

Upon introduction of KOOS, the developers reported its test-retest reliability, construct validity, and responsiveness to clinical change (e.g., surgery, physical therapy) for young and middle-aged participants before and after ACL reconstruction [42]. Subsequent numerous studies on KOOS for young and elderly groups further confirmed its internal consistency, content validity, test-retest reliability, construct validity, and responsiveness after knee injuries and/or osteoarthritis development [43]. Among the subscales, content validity of ADL, Sport/Rec, and Pain subscales was better for old individuals, young individuals, and individuals with painful knee conditions, respectively [43].

Based on the results of KOOS reported by a group of competitive athletes who had undergone ACL reconstruction, Salavati et al. [44] stated that all items of KOOS were highly correlated with their hypothesized subscale (internal consistency) and in almost all cases, these correlations were stronger than the correlations between each item and the other remaining subscales (dimensionality). Furthermore, after analyzing the test-retest reliability, ceiling, and floor effects, and construct validity, the authors confirmed the validity and reliability of KOOS for competitive athletes after ACL reconstruction [44].

2.3 Biomechanics of Horizontal Hop Tests

Numerous studies have been conducted using the motion-capture system, to better understand the kinematics of the horizontal hop tests and the compensatory mechanisms that the injured limb develops following an injury. A number of these studies are reviewed in this section.

In order to investigate the compensatory mechanisms adopted during the landing phase of hop tests in the presence of thigh muscles weakness, Orishimo and Kremenic [40] designed a study in which able-bodied individuals achieved equivalent single-leg hop distance, before and after a thigh muscles fatigue protocol. As the authors expected, the landing biomechanics was significantly altered in the fatigued state, which was proposed to induce temporary quadriceps weakness (a common lower limb deficiency in ACL reconstructed patients). These alterations were listed as

increased knee ROM, increased ankle plantarflexion moment, and variations in the pattern of sagittal ankle angles during landing while the ankle ROM, ground reaction forces and maximum total support moment (defined as the sum of the hip, knee, and ankle net moments along each trial) remained unchanged. The authors stated that greater knee flexion was the result of the longer time that the participants required to decelerate the center of mass at a fatigued state. Additionally, the unchanged ground reaction forces and maximum total support moment were the results of equivalent hop distances in fatigued and unfatigued states. Therefore, the increase of ankle plantarflexion moment could compensate for the knee muscle deficiencies and keep the maximum total support moment unchanged [40].

In their subsequent study [20], Orishimo et al. studied side-to-side sagittal biomechanical differences of ACL reconstructed patients with LSI values over 85%, during takeoff and landing periods of the single-leg hop. The results showed 25% and 18% reduction in knee ROM of the injured limb compared to the uninjured limb during takeoff and landing periods, respectively, while the ROM of hip and ankle also tended to be smaller for the injured limb during both takeoff and landing. The knee ROM reduction during the takeoff was accompanied by over 38% decrease in peak knee moment and power and was compensated by 38% and 21% increase in peak moment and power of the hip. The knee ROM reduction during the landing was accompanied by 43% decrease in knee power absorption and was compensated by 42% growth in peak power absorption of the ankle. The authors interpreted the compensatory mechanism of the ankle during the landing as a strategy developed for softer landing on the injured leg. Furthermore, based on the compensations by both hip and ankle, the authors declared that the single-leg hop is a measure of total lower limb function rather than the knee function alone [20].

Augustsson et al. [37] suggested a novel and reliable fatigue protocol based on 50% and 80% of one-repetition maximum weight (referred hereafter as 50% strength and 80% strength states, respectively) to investigate its effects on the sagittal kinematics and kinetics of takeoff and landing phases of the single-leg hop among able-bodied individuals. While the hop distance significantly decreased for the fatigued states, sagittal knee and hip ROMs were also significantly reduced for both fatigued states during the takeoff. Therefore, the participants had a more upright posture, leading to shorter hop distances. During the landing, hip ROM decreased significantly for the 80% strength state to adapt to the high demand landings [37].

In a study conducted by Gokeler et al. [21], early muscle activation of the injured limb was described as a strategy to provide higher knee stability and limb stiffness during the landing phase of the single-leg hop test. Side-to-side comparison of the lower limb joints among the patients 6 months post ACL reconstruction showed decreased ROM in all joints of the injured leg during the take-off while this reduction was significant for the knee. Although not significant, a similar trend was also observed during the landing period for the knee and hip of the injured side, which could be a result of knee stiffening strategy during the landing. However, the ankle ROM of the injured side was significantly greater than the contralateral side during the landing period [21].

Wren et al. [19] compared sagittal biomechanics of three groups of uninjured participants, symmetrical ACL reconstructed participants (hop distance LSI > 90%) and asymmetrical ACL reconstructed participants during takeoff and landing phases of single-leg hop tests. The results of the takeoff phase for asymmetrical participants demonstrated smaller knee and hip ROMs for the injured side compared to the uninjured side and smaller ankle ROM compared to uninjured participants while the symmetrical participants also showed the latter difference. During the landing, smaller knee and hip flexion angles, and larger ankle plantarflexion were obtained for the injured side of the asymmetric participants compared to their contralateral leg. Based on the observation of reduced knee energy absorption and flexion moment during landing, the authors concluded that both symmetrical and asymmetrical participants tried to offload their injured knee and shift the load to the hip and ankle, respectively, to have a stiffer landing pattern. Also, it was notable that the symmetrical participants had gained symmetry in hop distance partly by shorter hop distances attained by their uninjured limb. Therefore, the authors concluded that biomechanics of hopping should be considered in addition to LSI values for clinical decision making regarding RTS [19].

Xergia et al. [16] reported side-to-side and between-groups differences in sagittal hop kinematics among uninjured and ACL reconstructed participants 6 to 9 months post-surgery. According to their results, the injured group had smaller knee and ankle peak flexion and dorsiflexion angles on their injured limb compared to the uninjured limb during both propulsion and landing phases of the single-leg hop, TSLH, and crossover hop tests. Additionally, the injured group demonstrated a smaller ankle peak dorsiflexion angle during the propulsion phase and a greater hip peak flexion angle during the landing phase on their injured limb, compared to the

uninjured group. The authors mentioned that by reducing the flexion of knee and ankle, the injured participants could have a stiffer landing pattern accompanied by pre-activation of limb muscles to attain more stability before and during the landing. The authors emphasized that it is not clear how this compensatory mechanism would alter ACL loading, however reducing knee flexion during the propulsion phase would result in reduced hop distances and subsequently, reduced landing forces. The distance-related LSI values for the injured group of this study were significantly lower than the uninjured group [16].

In order to investigate the effect of quadriceps muscle strength asymmetry on the functional performance at the time of RTS, Schmitt et al. [7] compared a group of ACL reconstructed participants who were cleared for RTS with a group of uninjured participants during the single-leg hop, TSLH, crossover hop and timed hop tests. They found that the ACL reconstructed group obtained significantly lower LSI values on all hop tests compared to the uninjured participants. This difference was originated from shorter distances hopped on the injured side among the ACL reconstructed group. The ACL reconstructed participants who had asymmetrical quadriceps strength (LSI<90%) showed greater hop asymmetry in crossover and timed hop test, compared to the uninjured group, and greater hop asymmetry in the single-leg hop and TSLH compared to those of ACL reconstructed participants who had symmetrical quadriceps strength (LSI>90%). The authors concluded that quadriceps strength deficiency could negatively influence hop performance. Additionally, the authors stated that as a consequence of weakness in quadriceps muscles, movement patterns can be altered and cause cartilage damage development due to excessive load transferring at knee joint surfaces [7].

In an attempt to investigate the effect of leg dominancy on kinematics and kinetics of the single-leg hop test, Van der Harst et al. [45] reported no significant difference between dominant and contralateral leg of able-bodied athletes except for hopped distance and hip maximum extension angle, resulting to a more upright posture after landing with non-dominant leg compared to the dominant one. Also, by observing similar peak joint angles, ground reaction forces, and joint moments for both legs, the authors concluded that the non-injured leg of the patients following knee injuries could be considered as the reference leg, without consideration of its status as dominant or non-dominant. By comparing hop distance of single-leg and TSLH test for three groups of uninjured, recently ACL reconstructed (13 weeks post-surgery) and formerly ACL

reconstructed (54 weeks post-surgery) occasional exercisers, Petschnig et al. had also concluded that regardless of the dominance, the uninjured leg can be used as a reference control leg during these tests [35].

In a systematic review and meta-analyses of biomechanical alterations observed in single-leg hop test performance of ACL reconstructed participants, Kotsifaki et al. [46] reported smaller knee ROM, peak knee flexion angle, and peak ankle dorsiflexion angle, smaller knee and hip peak flexion moments, smaller knee power absorption, and larger ankle power absorption for the injured limb compared to contralateral limb during propulsion and landing. There was no difference between vertical ground reaction force for injured limb compared to the contralateral limb. The authors also reported smaller peak knee flexion angle and moment, and knee ROM for the injured limb compared to uninjured participants during propulsion and landing. Kotsifaki et al. associated the smaller knee flexion angles of the injured limb with altered quadriceps activation and decreased quadriceps strength, leading to stiffer and more upright landings that increase the stress on the ACL. While the kinematic differences between injured and uninjured leg groups were reported to be small (not detectable with the naked eye) and need further investigation to determine their clinical importance, the authors suggested biomechanical monitoring of the hop tests, as symmetrical hop distance could not guarantee symmetrical and unimpaired biomechanics of hopping.

2.4 Kinematic Measurements of Human Locomotion

2.4.1 Global and Local Frames

Quantitative biomechanical movement analysis and collecting interpretable numerical information about the musculoskeletal system require the definition of various global and local frames, which correspond to the measurement systems, analysis techniques, and the body segments to be analyzed [47]. For human movement analysis, the International Society of Biomechanics (ISB) suggests the consideration of Motor Task Frame, an orthogonal global frame in which the X-axis points the direction of the progression during the locomotive tasks, Y-axis is vertical and points upwards, and Z-axis points to the right [48]. To study the kinematics of joints and body segments with high inter- and intra-participant repeatability and interpretable outcomes, local anatomical frames are defined based on bony anatomical landmarks [49–51] in a way that anatomical axes mostly associate with the anatomical planes (sagittal, transverse, coronal) for each

body segment. Other technical frames such as Marker Cluster Technical Frame (used in motion-capture analysis) and Sensor Technical (or Inertial) Frame (used in IMU analysis) are definable based on the nature of analysis [47].

According to classical mechanics, the coordinate of a particle can be transformed between a local frame and a global frame based on Eq. (4):

$$p^G = R_L^G . p^L + o^G \tag{4}$$

where p^G and p^L denote the position of the particle in global and local frames, respectively; o^G stands for the position of the local frame's origin with respect to the global frame and R_L^G denotes the rotation matrix of the local frame with respect to the global frame. The columns of R_L^G are mutually orthogonal unit vectors, defining the orientation of the axes of the local frame with respect to their corresponding axes of the global frame [47].

2.4.2 Joint Coordinate System

In order to describe the relative translation and rotation of proximal and distal bony segments, various mathematical representations have been implemented [47,50,52]. Cardan/Bryant angles (also called Euler angles in the literature, specifically when the first and last rotation axes are the same) were used mainly in the past to express the relative rotation of two adjacent segments. However, these angles depend on the sequence of rotations around the three axes and prone to the occurrence of singularity condition (gimbal-lock) [47,50,52]. Without having the mentioned problems, helical angles can be the alternative for Euler angles; however, they are highly sensitive to the measurement errors and noise inherent with photogrammetric and electrogoniometric data reconstruction [52]. To avoid these shortcomings and report the results of movement analysis in an interpretable fashion for the clinicians, the joint coordinate system was defined by Grood and Suntay [50]. This coordinate system is composed of two body fixed axes embedded in the distal and proximal segments, and a floating axis which is commonly perpendicular to both body fixed axes at every time instant. Therefore, the nonorthogonal coordinate system, which was initially defined for the knee by Grood and Suntay [50], can describe the joints rotations, regardless of their order of occurrence, and hence provides a standard language for the communications among clinicians and engineers. ISB has further expanded the definition of joint coordinate system for the knee to the other joints, such as hip and ankle [51].

2.4.3 Stationary Motion-Capture Systems

Motion-capture systems are the stationary systems that can track the 3D position of passive (reflective) or active (light-emitting diodes) markers that are attached to the anatomical landmarks, within a restricted experimental volume [53]. These systems are the gold standard for the measurements of 3D position and orientation of human body segments [54]. If the errors originated from soft tissue artifacts can be assumed negligible, the accuracy of these systems for position and segments orientation measurement can be better than 0.2 mm and 0.6 degrees, respectively [55]. However, by using motion-capture cameras, kinematic measurements of human movement should be performed in a restricted experimental volume within advanced labs, and can barely reflect the participants' performance of in-field functional activities or longer gait trials. Furthermore, the in-lab systems are expensive, complicated to be operated, and can interfere with the activity performance [23,56].

2.4.4 Wearable IMU systems

IMUs are ambulatory wearable measurement systems that have been introduced to the field of human movement analysis after the development of powerful microcontrollers, high capacity memories, small and long-lasting batteries, and miniature sensors [57]. These systems are composed of accelerometers, gyroscopes, and in some cases magnetometers, to measure acceleration, angular velocity, and magnetic field, respectively, in their own three-dimensional technical frame. By using a proper sensor-to-segment calibration method (described in Section 2.5.1.1), IMUs' data can be used to find acceleration and angular velocity of body segments. In contrary to motion-capture systems, IMUs are compatible with in-field sports movement analysis, and provide advantages such as detailed monitoring with minimal interference with athletic tasks, being portable as attachments to clothing and sports equipment, and compatibility with various outdoors conditions (e.g., weather, light, etc.) [55].

2.5 Human Locomotion Kinematic Measurements with IMUs

2.5.1 Joint Angles Quantification with IMUs

Calculating the orientation of the body segments with IMUs is composed of three main steps: (1) alignment of the sensors' technical frame with the anatomical frame of the corresponding segment (sensor-to-segment calibration), (2) estimating initial orientation of the segments, and (3) estimating the instantaneous orientation of the segments along the activity [55]. Errors and drifts

originated at each of these steps can affect the accuracy and precision of the estimated orientations and subsequent joint angle calculations. The sources of error and major approaches for the accomplishment of each step are discussed in the following sections.

2.5.1.1 Sensor-to-Segment Calibration

A preliminary requirement for the 3D joint angles calculation is that the orientations of the proximal and distal segments are known with respect to a common reference frame [50]. However, IMUs measure the angular velocity and acceleration in their own technical frames [58]. Although the relative orientations of the sensors' technical frames might be known if magnetometers are being used, they do not clinically represent the relative orientations of the segments, to which sensors are attached. Therefore, several sensor-to-segment calibration procedures based on uniaxial functional tasks and simple postures are presented in the literature [22,58–60] to transform each sensor frame to its corresponding anatomical frame. The joint coordinate system of each joint can be later defined based on the embedded anatomical axes of the two segments and a floating axis, as discussed in Section 2.4.2.

Favre et al. [22] proposed a functional alignment method for shank and thigh, which used the gravity vector to align the vertical axis of the sensor frames during the standing posture. For the alignment of sensors' axes in the horizontal plane, a hip abduction/adduction was performed while the knee was locked during this movement to ensure that the angular velocities recorded for the two segments were equal in a common reference frame. Although the authors obtained mean errors less than 3.5 degrees for 3D joint angles estimation during short walking trials [22], the calculated angles were not clinically reliable and meaningful as they did not correspond to the segments' anatomical axes [59]. Therefore, the authors proposed a subsequent 4-step procedure to transform the technical frames of the thigh and shank sensors to their corresponding anatomical frames [59]. First, a hip abduction/adduction was performed actively by the participant to align the technical frame of the thigh sensor with the frame of the shank sensor. Then, a passive knee flexion/extension and a shank rotation movement in the frontal plane were performed by an examiner while the participant was at a sitting posture. Through these two functional tasks, the two anatomical rotation axes of the shank were obtained and used to build up the anatomical frame of this segment. Finally, a static stance trial was performed to assign zero knee angles to this posture and remove the angular offset to enhance the agreement of the measured joint angles with

clinical conventions [59]. The implementation of this sensor-to-segment calibration method showed high repeatability in the estimation of 3D joint angular patterns, and the mean errors of 3D joint angles estimation during gait trials were less than 8.5 degrees [59]. Since Favre et al. did not propose any method for calibration of pelvis sensor and their calibration method for the thigh sensor depended on the calibration of shank sensor, Nazarahari et al. [58] proposed a sensor-to-segment calibration procedure that can be used for calibration of pelvis, thigh, shank and foot segments. The calibration procedure proposed by Nazarahari et al. (our research group) consisted of a 5-second quiet standing posture, followed by 10 repetitions of hip flexion/extension. The participants were instructed to lock their knee and ankle joints during flexion/extension and try to have a planar motion of their leg, with self-selected speed and range of motion [58]. In addition to showing the highest inter-participant repeatability compared to the sensor-to-segment calibration methods presented in [59,60], Nazarahari's algorithm could suppress mean RMS errors of 3D joint angles estimation during gait trials to less than 8 degrees [58]. As these results showed to be promising in the alignment of sensors' technical frames with lower limb segments' anatomical frames, we adopted the procedure presented in [58] for sensor-to-segment calibration prior to TSLH tests.

2.5.1.2 Estimating Initial Orientation of Segments

Although accurate estimation of initial orientation has received less attention in the literature, it can considerably affect the estimation of the orientation during the activity (i.e., decreasing/increasing the offset error) [55]. A commonly suggested approach for initial orientation estimation uses the gravity vector to find the segments' tilt during an initial motionless period and assumes the heading of all segments to be aligned with the direction of locomotion [23,55]. While accelerometer can be used as an inclinometer when the body acceleration is negligible compared to gravity, IMUs have no component which is sensitive to the heading angle [59], and the latter assumption on segments' heading can add errors to the results.

2.5.1.3 Estimating the Instantaneous Orientation of the Segments along the Activity

Strap-down integration of the segments' angular velocity is one of the main approaches to calculate the instantaneous segments' orientation. However, integration of the IMUs' signals is accompanied by drift accumulation, which mainly originates from electronic bias error and deviations from the sensing axes [56,57]. The proposed algorithms in the literature rely on two

drift reduction methods. The first method uses the biomechanical constraints of the motion, such as motionless periods and cyclic nature of gait for drift reduction. The second method implements sensor fusion techniques such as Kalman filter and virtual shifting of the sensors to the joint center of rotation for drift estimation [54]. A combination of these methods might also be effective, considering the dynamics of the motion.

In order to avoid integration and subsequent accumulation of the drift, Dejnabadi et al. [57] virtually shifted the shank and thigh IMUs to the knee center of rotation and assumed that the virtual acceleration vectors were equal in magnitude while their deviation angle represented the knee angle. Based on this method, the accurate position of the sensors was required to calculate virtual accelerations at the knee joint and was obtained based on photos taken in the sagittal plane from each participant. Although the authors concluded that with this method, absolute knee angles in the sagittal plane could be estimated for any arbitrary movement, it is notable that this method cannot estimate thigh and shank orientations with respect to a fixed global frame [56]. Furthermore, the RMS error of 1.3 deg and correlation coefficient of 0.997 that were reported in comparison to the knee angles obtained with an ultrasonic motion measurement system deteriorated in higher walking speeds. Therefore, the assumption of fixed knee center of rotation might not be valid throughout the highly dynamic activities [57]. In an attempt to expand their method for ankle angles, Dejnabadi et al. [56] found the low acceleration periods (foot-flats) to estimate the shank inclination based on gravity vector. As such, the difference between ankle angle (estimated with virtual acceleration vectors) and the inclination angle of the shank (estimated with gravity vector) was regarded as shank's orientation drift during foot-flat periods. The unknown drift during high acceleration periods was then estimated with the application of a piecewise cubic Hermite interpolation, and subtracted from the obtained segments' orientations. This de-drifting by the use of biomechanical constraints of gait resulted in RMS errors of 1 and 1.6 deg in the estimation of knee and ankle angles, respectively, and was reported to be suitable in clinical monitoring of 2D (two-dimensional) joint angles [56].

In a method similar to [56], Fasel et al. [55] shifted the accelerometer readouts of the proximal and distal segments to the joint center of rotation to estimate the angular drift induced following the strap-down integration of the segments' angular velocities. Therefore, the difference between the virtual joint accelerations calculated based on each of the connecting segment's acceleration

was regarded as the drift. Fasel et al. applied their algorithm for indoor carpet skiing and used the data of highly dynamic periods for drift estimation to obtain a high signal to noise ratio [54,55]. Based on their findings, not only the magnitude of the drift increased linearly over time, but also oscillated around this linear increase, proportionally to the turns that athletes had to make along the ski path. Accuracies, precisions, and correlation coefficients of their proposed 3D joint angles algorithm for finding the trunk, hip, and knee angles were better than 11 deg, 5 deg, and 0.7, respectively, during 2-minute carpet skiing trials. The authors pointed out that drift accumulation is positively proportional to the volume of measurement, joints range of motion, and duration of the measurement, while the growth of orientation drift might be acceptable for short activities (< 30 seconds) [54,55]. In their next study, Fasel et al. tested the efficacy of their algorithm during outdoor skiing on a slalom with 26 deg of inclination [54]. Six video cameras that could only record the kinematics in 2D (an approximation of sagittal plane) were used as the reference system. By the implementation of their algorithm and sensor fusion methods, the authors de-drifted the sacrum sensor based on the acceleration signal of all adjacent sensors (i.e., sensors attached to the sternum, right thigh, and left thigh). Subsequently, the de-drifted sacrum sensor was used for drift reduction of the remaining sensors and resulted in accuracy and precision higher than 13 deg and 6 deg, respectively, for the sagittal hip and knee angles [54]. The authors declared that highly flexed joints required for ski maneuvers could increase the misalignment of technical frames' and anatomical frames' axes and hence contribute to the growth of joint angles errors. Furthermore, sensor wobbling and soft tissue artifacts during highly dynamic activities could alter the orientation of the sensor with respect to the body segment [54].

By exploiting the kinematic constraints of the knee joint (i.e., considering the knee as an approximate hinge joint and assuming the major rotations of knee joint to be about its mediolateral axis) and attributing the knee joint angular velocity to both shank and thigh angular velocities, Seel et al. [28] obtained the longitudinal axes of the segments with respect to the technical frames and calculated sagittal knee angle accordingly. Therefore, no additional sensor-to-segment calibration was needed, and the gyroscopes data could be used during the first few seconds of walking to find longitudinal anatomical axes of the thigh and shank. Furthermore, by virtually shifting the accelerometer data of both segments to the knee center of rotation (as an unknown point), the position of knee center of rotation with respect to the IMUs could be obtained. By applying this algorithm for both limbs of a transfemoral amputee, the authors found the accuracy of the sagittal

knee and ankle angles to be 0.7 and 0.8 deg during walking trials for the prosthetic limb while the knee and ankle angle errors of the intact limb were equal to 3.3 and 1.6 deg, respectively. Since the anatomical markers of the reference system were directly applied on anatomical landmarks of the intact side, Seel et al. concluded that by applying the markers on sensor boxes and virtually reconstructing the anatomical markers, one would underestimate the joint angle errors and ignore the soft tissue artifacts and non-rigidity of the segments [28]. The authors further stated that the errors of their suggested algorithm might grow in the presence of notable mediolateral acceleration, which happens during sport maneuvers [28,54].

Rouhani et al. [23] used a system of 4 IMUs to find 3D joint angles of multi-segment foot and ankle complex during 5-minute straight walking trials, using forward and backward strap-down integration. By thresholding the accelerometers' readouts, the authors found quasi-static instants within the stance phase of each gait cycle and used the gravity vector to find segments' tilts while segments' heading angles were assumed to be zero. The strap-down integration was updated at every gait cycle and minimized the mean RMS errors of estimated joint angles to less than 1.2, 1.4, and 2 deg during slow, normal, and fast walking, respectively. Mean ROM errors below 4 deg for all anatomical planes, speeds, and joints, as well as mean correlation coefficients of above 0.82 for all these cases, further confirmed the validity of the proposed method against a motion-capture system. Based on the estimated joint angles, Rouhani et al. found significant reductions in the joints' ROM of the patients with ankle osteoarthritis compared to able-bodied participants [23].

2.5.2 Temporal Events Detection with IMUs

Temporal events detection with IMUs has been performed to obtain stride time, stance time, and subdividing events of the stance phase by feature detection methods applied on foot, thigh, and waist acceleration signals; as well as foot, shank, and thigh angular velocity signals, and a combination thereof [29]. During gait, initial foot-ground contact (IC) and terminal foot-ground contact (TC) instants are equivalent with heel-strike and toe-off instants and are accompanied with the appearance of peaks in shank and foot pitch angular velocity signals [25–27], which can be used to find these temporal events.

Given that the magnitude of the IC- and TC-related peaks might alter with characteristics of gait trials, a gait events detection method in time-frequency domains was proposed by Aminian et al. [27]. Through multi-resolution decomposition of the shank pitch angular velocity with a Coiflet

wavelet, high-frequency artifacts and drifts of the signal were canceled prior to the kinematic feature detection. The local minima pertaining to temporal events were then searched within appropriate time windows and specific frequency ranges of the original signal. Comparison of the identified temporal events with results of toe- and heel-attached force-sensitive resistors showed no significant error in toe-off detection and a systematic 10-ms delay for heel-strike detection [27].

To enhance temporal events detection based on shank pitch angular velocity signal, Salarian et al. [26] relied on the global positive peak of each gait cycle, standing for approximate mid-swing instants of that cycle. The two local minima discussed by [27] were then searched within 1.5-second time windows, defined at both sides of the mid-swing instant. Since a clear local minimum might not be detectable within the pre-swing time window due to smooth movements at the time of foot-ground terminal contact, further refinement of peak detection algorithm was suggested by the authors, by implementing a low-pass filter and introducing peak-height thresholds for accurate detection of TC instants. By implementing both Aminian's [27] and their proposed algorithms, Salarian et al. reported improvements in systematic errors of IC and TC detection (31% and 56%, respectively) compared to Aminian's algorithm [27], and attained mean errors less than 9 ms for gait temporal events detection. They also reported 13% and 8% improvement in the standard deviation of IC and TC detection errors, respectively, and attained precisions better than 27 ms in gait temporal events detection.

In contrast to the discussed methods that used shank pitch angular velocity for temporal events detection, Selles et al. [61] used the acceleration components of the shank to find IC and TC instants during gait. By categorizing the gait cycles into fast and slow strides based on approximate stride durations, appropriate cut-off frequencies for filtering of the shank acceleration signals were defined to adapt to the frequency content of the performed gait trial. IC and TC instants were then found through peak detection algorithms applied on longitudinal and frontal acceleration signals of the shank, and resulted in error means of less than 35 ms in gait temporal events detection for transtibial amputees and able-bodied participants [61].

In addition to heel-strike and toe-off instants, heel-off and toe-strike events have also been of interest to the studies [25,29] that aimed to find the foot-flat portion of the stance-phase, as a relatively motion-less interval required for the gait trajectory tracking algorithms. In this light, Sabatini et al. [29] used thresholding, peak detection, and zero-crossing of the foot pitch angular

velocity signal to find sub-phases of the stance during inclined walking. However, they only reported the errors of heel-strike and toe-off detection (mean errors of 2 ms and 35 ms, respectively) compared to a system of footswitches.

Mariani et al. [25] attempted to find the sub-phases of the stance phase by an IMU attached to the forefoot of the participants and finding the maxima, minima, and zero-crossings of the pitch angular velocity, time derivative of the angular velocity norm, norm of the acceleration, and absolute value of the time derivative of acceleration norm signals that could be related to toe-off, heel-strike, toe-strike, and heel-off events. The reference system that the authors used for their temporal events detection algorithm was a system of pressure insoles with thresholds at 5% of the bodyweight over the forefoot and hind-foot regions to find temporal events of each gait cycle. Through a meticulous search of kinematic signal features, mean errors less than 4 ms and standard deviations less than 54 ms were obtained for best signal features proposed for each of the four temporal events. Mariani concluded that acceleration signals provide better features for detecting major temporal events (i.e., heel-strike and toe-off) while angular velocity-based features facilitate the detection of minor temporal events (i.e., toe-strike and heel-off) [25].

2.5.3 Spatial Parameters Quantification with IMUs

The implementation of indirect methods of gait trajectory tracking with IMUs, which rely on the parameterization of trunk and foot acceleration signals and angular rotations of the body segments, has led to erroneous estimations that originate from physiological variability among the participants [29,62]. The direct methods suggest double integration of the gravity-free acceleration of each segment and emphasize the importance of optimal estimation of segments' orientation and initial conditions, compensation for the IMUs offsets and sensitivity drifts, and validity of the biomechanical assumptions to reach an acceptable accuracy in gait trajectory tracking [24,29]. However, the effective removal of thermal-mechanical and electronic noise of accelerometers and gyroscopes to prevent the unbounded propagation of errors after integration is complicated due to the nonlinear relationship between noise and integration time [63]. The reviewed studies in this section shed some light on the complexities of human trajectory tracking with IMUs and provide practical solutions to minimize the aforementioned errors.

In order to analyze the sagittal trajectory of the foot during treadmill walking, Sabatini et al. [29] used the direct methods to find foot tilt, walking speed, and stride length. According to their

approach, the slope of the walking platform could be estimated based on the frontal and vertical acceleration readouts of the foot-mounted IMU during the initial foot-flat interval and corrected thereafter, to provide the initial orientation of the foot at each gait cycle. After compensating for the gyroscope's offset by deducting the mean pitch angular velocity of the initial static stance from the entire signal ("nulling algorithm"), the instantaneous foot orientation could be obtained through strap-down integration and be used for gravity-cancellation of the foot accelerometer readouts. Subsequently, double trapezoidal integration of the gravity-free acceleration was accompanied by an intermediate step of velocity correction, (assuming a linear corrective function to remove accelerometer's electrical noise) to estimate foot tilt and walking speed with 1.52% and 1.8 km/h error, respectively. Sabatini concluded that resetting the strap-down integration based on the cyclic nature of gait and correcting the orientation of the mid-stance phase based on gravity vector is effective in suppressing the growth of unbounded errors, originated from the IMUs drifts [29].

By implementation of a similar method and using the cyclic nature of the gait, Sabatini [62] presented an algorithm to estimate the planar trajectory of a synthetic gait trial in the presence of thermal deviations from the calibration reference temperature and for a range of gyroscope and accelerometer noise. In addition to the de-drifting methods that Sabatini had used to cancel orientation's drift in [29], he applied a spherical linear interpolation function to achieve equal initial and ending conditions (for both orientation and linear velocity) at each gait cycle. Sabatini reported the RMS errors of the orientation estimation and sagittal trajectory tracking to be 14.6 deg and 17.7 cm, respectively, when the strap-down integration was updated at every gait cycle. By applying strap-down integration at every two gait cycles, the RMS errors of the orientation estimation and sagittal trajectory tracking grew to 14.8 deg and 30.0 cm, respectively. Hence, the author concluded that the accuracy of trajectory estimation considerably depended on the length of the time window over which strap-down integration was applied [62].

Using the same concept of periodical drift correction at foot-flat intervals, Mariani et al. [24] proposed a new method of velocity correction to estimate 3D foot trajectory of young and elderly participants, performing U-turn, 8-turn, and 6-minute straight walking trials and compared the results with the gold standard of the motion-capture system. Based on this algorithm, foot angular velocity signal was used to find the stance periods, and continuous intervals of low angular velocity norm within the stance periods were regarded as the foot-flat intervals. Mariani then updated the

initial orientation of the foot at the mid-point of foot-flat intervals by finding the foot tilt based on the gravity vector and setting the foot heading angle equal to the heading of the previous time sample. Through this method, the authors could track the foot orientation along the turns at which the heading angle cannot be ignored as in straight walking. As a preliminary step for gravity cancellation, Mariani et al. applied the strap-down integration over each gait cycle to find foot orientation with respect to the lab fixed global frame, used the foot orientation to isolate the foot body acceleration form gravitational component of the acceleration, and integrated the former to obtain foot velocity. As the linear foot velocity is accompanied by a considerable amount of drift at this stage, the authors proposed a corrective sigmoid-like p-chip interpolation function to be deducted from the foot velocity during each gait cycle and ensure zero-velocity of the foot at foot-flat mid-points while correcting the foot linear velocity at every time instant. Trapezoidal integration was then applied to the corrected foot velocity to find foot trajectory. Although the authors observed significant differences between a number of IMU-based and camera-based gait parameters, their proposed algorithm could estimate stride length, stride velocity, foot clearance, and turning angle with mean (standard deviation) errors of 1.5 (6.8) cm, 1.4 (5.6) cm/s, 1.9 (2.0) cm, and 1.6 (6.1) deg, respectively, over the gait cycles [24].

Notably, all the discussed algorithms of gait trajectory tracking assume the velocity of the foot to be zero in a period or at a specific point during the stance phase [24,29,62,63]. Therefore, Peruzzi et al. [63] tested the validity of this assumption with a motion-capture system at three different gait speeds by attaching reflective markers to various anatomical landmarks of shank, forefoot, and hindfoot at popular locations of IMU attachment among the literature. The results showed that the zero-velocity assumption is only acceptable for foot landmarks and causes the stride length to be underestimated by less than 0.7%, whereas making the same assumption for shank landmarks enlarges the errors to about 3.3% of the stride length. Additionally, this assumption can be violated for higher gait speeds, where the stance phase becomes shorter. The authors stated that zero-velocity assumption during gait might be valid between 31% and 57% of the stance phase (regardless of the gait speed but depending on the attachment region). Calcaneus and lateral aspect of the rearfoot were regarded as the best IMU attachment regions for the validity of this assumption [63].

2.6 Functional Tests Kinematic Measurements with IMUs

While no study has attempted to use IMUs during horizontal hop tests, a few studies have used these wearable systems during vertical jumping tasks and are reviewed in this section.

Dowling et al. [30] applied three IMUs on the trunk, thigh, and shank of able-bodied individuals during unilateral and bilateral drop jump trials to assess the risk of ACL injury in this group and evaluate the capacity of IMUs to measure functional tests kinematics. Based on their method, the IC instant corresponded to the first peak of the shank vertical acceleration while the TC instant could be found based on the next occurring peak of the shank norm of acceleration signal. These temporal instants were further corrected to compensate for the systematic delay that the authors had identified in their events detection algorithm. Consequently, the jump height was calculated as a function of flight time by using ballistic equations, while the sagittal knee angle and trunk tilt were estimated based on sensor fusion algorithms. The implementation of this algorithm resulted in mean errors of less than 5 ms for temporal events detection, less than 6 cm for jump height estimation, and less than 8 deg for knee flexion and trunk tilt angles during various phases of drop jumps compared to the motion-capture and force-plate systems. According to these results and the fact that the IMUs system could differentiate between unilateral and bilateral drop jumps, the authors concluded that IMUs are promising tools to assess the risk of ACL injury, which is associated with smaller knee and trunk flexion angles during the landing [30].

Jakob et al. [31] focused on a range of dynamic activities that included walking, jogging, running, squats, and countermovement jumps to assess IMUs' efficacy in estimating sagittal knee angles. Relying on the proposed sensor-to-segment calibration method by Favre [22,59], the authors aligned the frames of the shank and thigh sensors and implemented an extended Kalman filter to calculate the sagittal knee angle during the activities. After removing the offset of joint angular curves obtained with IMUs and motion-capture system, Jakob et al. reported mean (standard deviation) of knee angles RMS errors to be less than 11(4) deg for all activities (7(3) deg for countermovement jumps). As was stated by Dejnabadi et al. [56], the performance of Kalman filter deteriorated for highly dynamic activities with centripetal acceleration components; however, the precision of the reported results by Jakob et al. seemed to be favorable, specifically for applications such as feedback training and performance evaluation [31].

Quagliarella et al. [32] used one triaxial accelerometer on the lateral side of each ankle to find the IC and TC instants during countermovement and squat jumps, performed by a group of able-bodied participants and a group of participants who had undergone surgery after Achilles tendon rupture. By applying a peak-detection algorithm on the norm of the accelerometer's signal within appropriate time windows, the authors found the IC and TC instants with errors less than 8 ms and 24 ms, respectively, after reducing the error of their temporal detection algorithm with corrective coefficients. The authors could also comment on the efficacy of jump performances, by integrating the accelerometer's signal during the flying phase and assuming this parameter to be associated with unnecessary limb rotations during flying phases [32].

Setuain et al. [33] used one IMU on the sacrum of ACL reconstructed handball players (on average, 6 years post-surgery) and uninjured handball players during vertical bilateral and unilateral drop jumps and vertical unilateral countermovement jumps to compare acceleration peaks, angular excursion, and jump phases duration between these two groups. Although the authors could identify differences in the mediolateral peak acceleration and angular excursion of the sacrum when the uninjured athletes switched to their contralateral leg to perform unilateral drop jumps, no significant difference was found for the investigated parameters between the injured and uninjured groups. The authors concluded that elite athletes might be able to restore their full jumping capacity after ACL reconstruction and acknowledged the usefulness of IMUs for assessing athletic tasks in clinics during the rehabilitation programs [33].

2.7 Summary of the Evidence and Importance of the Current Research

The studies reviewed in Section 2.3 emphasize the benefits of monitoring the kinematics of hop tests with motion-capture systems. Such detailed monitoring has enabled clinician-scientists to investigate compensatory mechanisms and kinematic deficiencies of injured and uninjured limbs. With the use of sophisticated stationary measurement systems, clinician-scientists have also studied injury mechanisms, differing effects on injured and uninjured limbs, and the association of hop kinematics with hop kinetics and other relevant clinical outcomes. As discussed in Sections 2.4 and 2.5, IMUs have become strong tools for ambulatory monitoring of gait kinematics, and numerous studies have been conducted to introduce IMU-based algorithms with high accuracy and precision for joint angles and temporospatial monitoring during human locomotion. The studies reviewed in Section 2.6 can be regarded as the pioneering studies that have incorporated IMUs

with vertical jumping functional tests. However, they have not assessed the capabilities of the IMUs in joint angular and temporospatial estimations during horizontal hop tests. Considering the frequency with which hop tests are used in clinical and rehabilitation settings and their importance as a criterion for RTS clearance, a study to develop and validate IMU-based algorithms to estimate kinematic outcomes of hop tests is lacking. Therefore, in Chapters 3 and 4, algorithms to obtain joint angles and temporospatial parameters of the TSLH test are provided and validated against a reference motion-capture system. These algorithms are also evaluated in a clinical research setting to compare hopping kinematics between youth with and without an intra-articular knee injury, and assess the association of hop kinematics and patient-reported clinical outcomes. By further improvement of the IMU-based kinematic algorithms in the future, low-cost widely available IMUs can be used by clinician-scientists to study various aspects of the hop tests (e.g., compensatory mechanisms, fatigue, joint coordination). Upon successful integration of IMU systems with clinical and rehabilitative protocols, these validated algorithms can assist in informing a timely RTS and early-onset osteoarthritis prevention in years following a knee injury.

Chapter 3

3 Quantification of 3D Joint Angles during TSLH Test with IMUs

The material covered in this chapter has been submitted as a research paper to the *Clinical Biomechanics* journal. The content of this chapter majorly remained identical with the submitted paper, while text formatting was conducted to fulfill thesis requirements of University of Alberta.

N. Ahmadian, M. Nazarahari, J. L. Whittaker, and H. Rouhani, "Instrumented Triple Single-Leg Hop Test: A Validated Method for Ambulatory Measurement of Ankle and Knee Angles using Inertial Sensors", submitted to *Clinical Biomechanics*

3.1 Abstract

Background: Hop tests are commonly used in clinical environments to measure function after sport-related knee injuries. Joint angles measurement during hopping is feasible in research-based environments equipped with motion-capture systems. Employing these systems in clinical research settings is inefficient, given the associated cost, preparation time, and expertise required to administer and interpret the findings. Therefore, this study aimed to introduce a wearable system comprising three inertial measurement units for 3D joint angular measurements during horizontal hop tests, validate the joint angles against a camera-based system, and evaluate its applicability in clinical research environments.

Methods: Ten able-bodied participants were outfitted with three inertial measurement units during triple single-leg hop trials. 3D knee and ankle angles were calculated using the strap-down integration method and results were compared with camera-based joint angles. Additionally, knee and ankle range of motion (ROM) during bilateral triple single-leg hop trials were compared for 22 participants with unilateral sport-related knee injuries and 10 uninjured participants.

Findings: Estimated angles had root-mean-square and ROM error medians of less than 2.3 and 3.2 degrees for both joints, and correlation coefficients of above 0.92 when compared with the camera-based system, for all hop phases. Injured participants had smaller sagittal ankle ROM on their injured side during the third hop (median (inter-quartile range) of 23.4 (8.3) for injured side

versus 25.8 (10.9) for uninjured side, p=0.008). Concurrently, they demonstrated smaller knee ROM symmetry indices (91.8 (34.2) for injured participants versus 111.3 (21.9) for uninjured participants, p=0.017) and injured knee sagittal ROM compared to uninjured participants (30.8 (10.4) for injured side of injured participants versus 36.4 (11.5) for both sides of uninjured participants, p=0.009).

Interpretation: The introduced system had appropriate accuracy to estimate hopping kinematics in a clinical research setting and reveal noteworthy differences in ROM of injured and uninjured samples.

Keywords: Knee injuries; Triple single-leg hop test; Joint kinematic analysis; Inertial measurement unit; Strap-down integration; Technical validation.

3.2 Introduction

Individuals suffering from severe knee injuries, such as meniscus and anterior cruciate ligament (ACL) tears are at 4-6 fold increased risk of developing osteoarthritis [64]. Alterations in joint loading following an injury can introduce compensatory mechanisms to overcome knee deficits [20]. The cumulative effect of these alterations, along with neuromuscular changes, and gains in adiposity might contribute to the development of future osteoarthritis [65,66]. Additionally, about half of athletes who tear their ACL fail to resume sports at their pre-injury levels, and the risk of reinjury or contralateral knee injury is substantial with a premature return to sport [9,67].

The distance achieved during a functional hop test has been shown to have good criterion validity to predict knee function in populations with severe knee injuries [14,68]. For a demanding test such as triple single-leg hop (TSLH), participants are required to control the movements of their body center of mass in both horizontal and vertical directions, using one leg only and maintain their dynamic stability after the last hop while preserving their momentum along the three hops [37,40,69]. Accordingly, this test can adequately reveal deficits, which may show up during challenging sports movements [45]. The outcome of the TSLH is typically expressed as a limb symmetry index (LSI) of total hopped distance, referring to the ratio of the total distance hopped on the involved leg over the corresponding distance, hopped on the uninvolved leg. LSIs of 85% or less in TSLH distance are considered abnormal [35] although higher LSIs do not guarantee

unimpaired hopping biomechanics. Due to the plausible changes in the neuromuscular control and strength of contralateral leg following an injury or the compensatory mechanisms developed by hip and ankle, knee deficits might be concealed when the total hop distance is solely recorded [19,20,38]. Consequently, numerous studies have used the motion-capture system to measure joint angles during the functional tests to gain better insight into lower extremity biomechanics following knee injuries [19,21,67,70].

Incorporation of the motion-capture system with the functional tests diminishes the most beneficial aspects of these tests such as requiring no specialized personnel, calibration time, participant preparation, and complex instrumentation, and will be limited to the sophisticated research laboratories. Therefore, an alternative measurement system, which can be optimally used for in-depth investigation of functional tests in clinical research settings is required. Inertial measurement units (IMUs) have been successfully used for able-bodied, clinical, and athletic populations to find the joint angles with high accuracies during the walking trials [23,28]. IMUs have also recently been applied to various vertical jumping studies [30,31,33] to calculate the joint angles and investigate the knee deficits, although their study populations were mostly composed of able-bodied individuals. To the authors' knowledge, no study has evaluated the capabilities of IMUs in the estimation of joint angles of injured or able-bodied participants during the TSLH; while camera-based studies [16,19] have widely reported significant intra-participant (side-to-side) and inter-participant (injured versus uninjured individual) differences among joints ROMs of these populations, when performing horizontal hop tests.

In this study, we have proposed a wearable system comprised of three IMUs per limb to calculate knee and ankle 3D joint angles during the TSLH and validated the outcomes with the gold standard motion-capture system (Technical Validation). The wearable system was then assessed in a clinical research setting for youth with a variety of sport-related intra-articular knee injuries and uninjured youth to evaluate its capabilities in detecting differences between hopping kinematics of the two groups during TSLH trials (Clinical Research Application). It was hypothesized that the wearable system can track the 3D knee and ankle joint angles with accuracies comparable to similar gait and jumping studies and reveal notable differences in hopping strategies between injured and uninjured leg groups.

3.3 Methods

3.3.1 Wearable Sensors System

3.3.1.1 Technical Validation Hardware

Three IMU modules (Physilog 3, Gait Up, Lausanne, Switzerland), consisting of a 3D accelerometer (range: ±11 g) and a 3D gyroscope (range: ±1200 °/s) were attached with double-sided hypoallergenic tape to the right thigh, shank, and foot of each participant (Fig. 4) and sampled the data at 500 Hz. For validation and calibration purposes, each IMU was equipped with three reflective markers attached to its box.

Fig. 4. Anatomical and sensor-box reflective markers, and the 3 IMUs, placed on the right thigh, shank, and foot of the participant for validation of the 3D knee and ankle angles estimated by the IMUs against the motion-capture system. Anatomical markers were removed after a 1-min upright standing still period was recorded with the cameras.

3.3.1.2 Clinical Research Application Hardware

Six IMU modules (Physilog 5, Gait Up, Lausanne, Switzerland) consisting of a 3D accelerometer (range: ±16 g) and a 3D gyroscope (range: ±2000 °/s) were attached with Velcro straps to the both thighs, shanks, and feet of the participants at the regions consistent with the Technical Validation (Table 1), and sampled the data at 256 Hz.

Table 1. Location of IMUs during both Technical Validation and Clinical Research Application studies, and location of anatomical markers during Technical Validation study. Axes of bony anatomical frames (BAFs) are defined based on anatomical markers of Technical Validation study.

	Segment		
	Thigh	**Shank**	**Foot**
IMU Location	Upper lateral thigh	Upper medial shank	Along the 2nd metatarsal
Anatomical Markers Location	Greater trochanter external surface (GT) Medial epicondyle apex (ME) Lateral epicondyle apex (LE)	Tibial tuberosity prominence (TT)* Medial malleolus apex (MM) Lateral malleolus apex (LM) Fibular head apex (HF)	Posterior calcaneal tuberosity (CA) Dorsum of 2nd metatarsal head (SM) Dorsum of 5th metatarsal head (VM)
BAF Axes Definition	Z-axis: Vector connecting ME to LE; positive direction from left to right X-axis: Perpendicular to the plane of GT, ME, and LE; positive direction in anterior direction Y-axis: Completing the orthonormal right-handed frame	Z-axis: Vector connecting MM to LM; positive direction from left to right X-axis: Perpendicular to the plane of HF, MM, and LM; positive direction in anterior direction Y-axis: Completing the orthonormal right-handed frame	X-axis: Vector connecting CA to SM; positive direction in anterior direction Y-axis: Perpendicular to the plane of CA, SM, and VM; positive direction in superior direction Z-axis: Completing the orthonormal right-handed frame

* A marker was placed on tibia but not used for this study.

3.3.2 The Reference System for Technical Validation

A stationary system of eight motion-capture cameras (Motion Analysis Corporation, Santa Rosa, CA, USA) was used as the gold standard for validation of knee and ankle joint angles during the Technical Validation study. This system recorded the position of anatomical markers (Table 1) and sensor-box reflective markers at 100 Hz and was synchronized with the IMUs using a stick poke to one of the sensor modules at the beginning and end of each trial. The stick was equipped with a reflective marker.

3.3.3 Experimental Procedure

3.3.3.1 Technical Validation Experiments

Ten able-bodied men with no history of acute knee injuries or musculoskeletal disorders were recruited through advertisements on the Univesity of Alberta campus. The participants were outfitted with the IMUs and reflective markers (See Sections 3.3.1.1 and 3.3.2) and were asked to stand still in their natural posture for 1 minute while both systems recorded their biomechanical data. Afterwards, the anatomical markers were removed to avoid hindrance during hopping, and the participants performed two trials of TSLH with their dominant leg, initiated and ending with 10-seconds standing still intervals. These motionless intervals were used to cancel the gyroscopes' drift along the corresponding TSLH trial.

3.3.3.2 Clinical Research Application Experiments

The wearable system of 6 IMUs (See Sections 3.3.1.2) was applied on a convenience sub-sample of 32 participants (11-19 years of age) from an ongoing prospective cohort study. This included 22 youth with time-loss, medical attention sport-related intra-articular knee injury (the injured group, hereafter referred to as G_I), and 10 uninjured youth (the uninjured group, hereafter referred to as G_{UI}). Knee injury was defined as a clinical diagnosis of knee ligament, meniscal, or other intra-articular tibiofemoral or patellofemoral injury that required both medical consultation and disrupted regular sports participation. G_{UI} was required to have no history of lower limb injuries to either leg. An experienced physiotherapist confirmed the eligibility of the participants to do TSLH trials based on two criteria: 1) participants' modified International Knee Documentation Committee (IKDC) knee examination (participants were required to have no knee effusion and to be able to straighten their knees to 0 degrees) and 2) injured participants' self-reported KOOS scores (participants were required to have no pain or difficulty with

twisting/pivoting in the injured knee and no difficulty in jumping on the injured knee). The age (on testing date), standing height (bare feet, using stretch stature method) and weight (bare feet with minimal clothing) of the participants were recorded prior to testing and the dominant leg of each participant was determined to be the one that they would use to kick a soccer ball as far as possible.

After outfitting the participants with the six IMU modules, they were asked to perform 20 repetitions of hip flexion/extension with their both legs while locking their knee and ankle in the natural configuration. This functional task was used to build up the mediolateral axis of each body segment, required for the sensor-segment calibration [58].

All participants performed two trials of TSLH with each leg, initiated and ending with 5-seconds standing still periods. The participants had to perform the hops consecutively and solidly stick to their last landing without excessive hops or the use of their contralateral leg, for a trial to be accepted.

Both parts of the study were approved by the ethics committee of the University of Alberta (Pro00065804 and Pro00063773), and all participants gave their informed written consent prior to their participation.

3.3.4 3D Joint Angles Estimation

To obtain the knee and ankle joint angles during TSLH using IMUs, the following steps were considered, similar to [23,24].

a) Sensor-Segment Calibration. In Technical Validation, anatomical markers were reconstructed at each time sample (i) using the sensor-box markers. The bony anatomical frame (BAF) of each segment (See Table 1 for the definition of BAF axes) with respect to the lab frame (LF) was expressed as $R_{BAF}^{LF}(i)$ at each time sample during the test. Sensors' technical frames (TFs) were expressed in relation to the lab frame as $R_{TF}^{LF}(i)$. Therefore, the TFs could be aligned with their corresponding BAFs using Eq. (5):

$$R_{TF}^{BAF}(i) = (R_{BAF}^{LF}(i))^{-1} \,.\, R_{TF}^{LF}(i) \tag{5}$$

In Clinical Research Application study, when the markers were not present, R_{TF}^{BAF} was obtained based on the IMU recordings during hip flexion/extension movements and upright static posture, according to [58].

b) Segments Orientation Calculation. The acceleration ($\overrightarrow{Acc}^{TF}$) and angular velocity ($\overrightarrow{Gyr}^{TF}$) measured by IMUs were first expressed in their corresponding BAF, using Eqs. (6) and (7):

$$\overrightarrow{Acc}^{BAF}(i) = R_{TF}^{BAF}(i) \,.\, \overrightarrow{Acc}^{TF}(i) \tag{6}$$

$$\overrightarrow{Gyr}^{BAF}(i) = R_{TF}^{BAF}(i) \,.\, \overrightarrow{Gyr}^{TF}(i) \tag{7}$$

In Technical Validation, $R_{BAF}^{LF}(0)$ was obtained once with cameras based on reconstructed markers and once approximated by calculating the initial tilt of each segment prior to hopping, using the gravity vector measured by accelerometer and assuming that the initial heading angles of all segments equal zero [23,55]. Obtaining $R_{BAF}^{LF}(0)$ with both these methods enabled us to analyze the effect of errors of initial orientation estimation on the accuracy of joint angles. In the Clinical Research Application, since no markers and cameras were present, only the latter method was applied to estimate $R_{BAF}^{LF}(0)$.

Then, a quaternion-based strap-down integration of $\overrightarrow{Gyr}^{BAF}$ was calculated according to [23,24] and $R_{BAF}^{LF}(i)$ was estimated based on $R_{BAF}^{LF}(i-1)$. Considering that each TSLH trial took only a few seconds, no corrective methods were needed to reduce the drift of gyroscopes [55].

c) Joint Angles Calculation. Knee and ankle joint angular curves at three anatomical planes during the TSLH trials were calculated in the joint coordinate system [50]. The angular curves were analyzed for each hop phase (Flying/Landing), based on the consecutive initial and terminal foot-ground contact instants detected by the motion-capture system.

3.3.5 Data Analysis

3.3.5.1 Technical Validation Data Analysis

To decrease the effect of morphological differences of participants on the accuracy of the wearable system, joint angle means of each hop phase were subtracted from the angular curves of the corresponding phase. The comparison between the two systems was made in terms of root-mean-square (RMS) error and correlation coefficient between pairs of angular curves during each

hop phase. Additionally, the knee and ankle ranges of motion (ROMs) were compared using both systems.

3.3.5.2 Clinical Research Application Data Analysis

The ankle and knee angular curves and ROMs were obtained during hop phases, which were split based on event detection algorithms, similar to [25,26,32]. The mean values (over the two TSLH trials) of ROMs in the sagittal plane were calculated and compared side-to-side for each participant and between the leg sub-groups of G_I and G_{UI}. Additionally, LSIs were obtained for the joints' ROMs of each participant, and the results were used for comparison of both G_I and G_{UI} groups. The normality of the population was tested using the Jarque-Bera test and rejected for a number of calculated parameters. Therefore, Wilcoxon signed-rank test and Wilcoxon rank-sum test were used, respectively, for the side-to-side comparison and the comparison between G_I and G_{UI} (α=0.05). Multiple comparisons were not used, as ROM of each joint during every hop phase was targeted as a potential TSLH outcome, and the purpose of comparisons was not to make clinical conclusions.

3.4 Results

Demographics of the participants who enrolled in Technical Validation and Clinical Research Application studies are shown in Table 2.

Table 2. Demographics of the participants enrolled in the Technical Validation and Clinical Research Application studies.

Characteristics	Technical Validation (n=10)		Clinical Research Application (n=32)	
	Injured (n=0)	Uninjured (n=10)	Injured† (n=22)	Uninjured† (n=10)
Sex (W/M)	-	0W/10M	17W/5M	9W/1M
Age* (years)	-	23 ± 3	16 ± 1	17 ± 2
Height* (cm)	-	177 ± 10	167 ± 12	171 ± 9
Weight* (kg)	-	68 ± 8	60 ± 14	65 ± 10
Dominant Leg (R/L)	-	10R/0L	19R/3L	10R/0L
Injured Leg (R/L)	-	-	12R/10L	-
Injured Leg (D/ND)	-	-	11D/11ND	-

n: Number of participants; W: Woman; M: Man; R: Right; L: Left; D: Dominant side; ND: Non-dominant side

†Injured and Uninjured participants of the Clinical Research Application study are referred to as G_I and G_{UI}, respectively, within the body of this chapter.

*Age, height, and weight are presented as median ± interquartile range among the participants.

All injured participants of this study had suffered from unilateral sport-related knee injuries within 15 months prior to the testing date.

3.4.1 Technical Validation Results

According to Fig. 5, visual inspection shows that the knee and ankle angular curves estimated for 10 able-bodied uninjured men (demographics in Table 2) with the wearable system were close to those measured with the camera system. When the segments initial orientations were estimated using cameras, the overall (all participants, anatomical planes, and hop phases) medians of RMS errors, ROM errors, and correlation coefficients were 2.2 deg, 2.6 deg, and 0.93 for the knee and 2.2 deg, 3.2 deg, and 0.92 for the ankle angular curves, respectively.

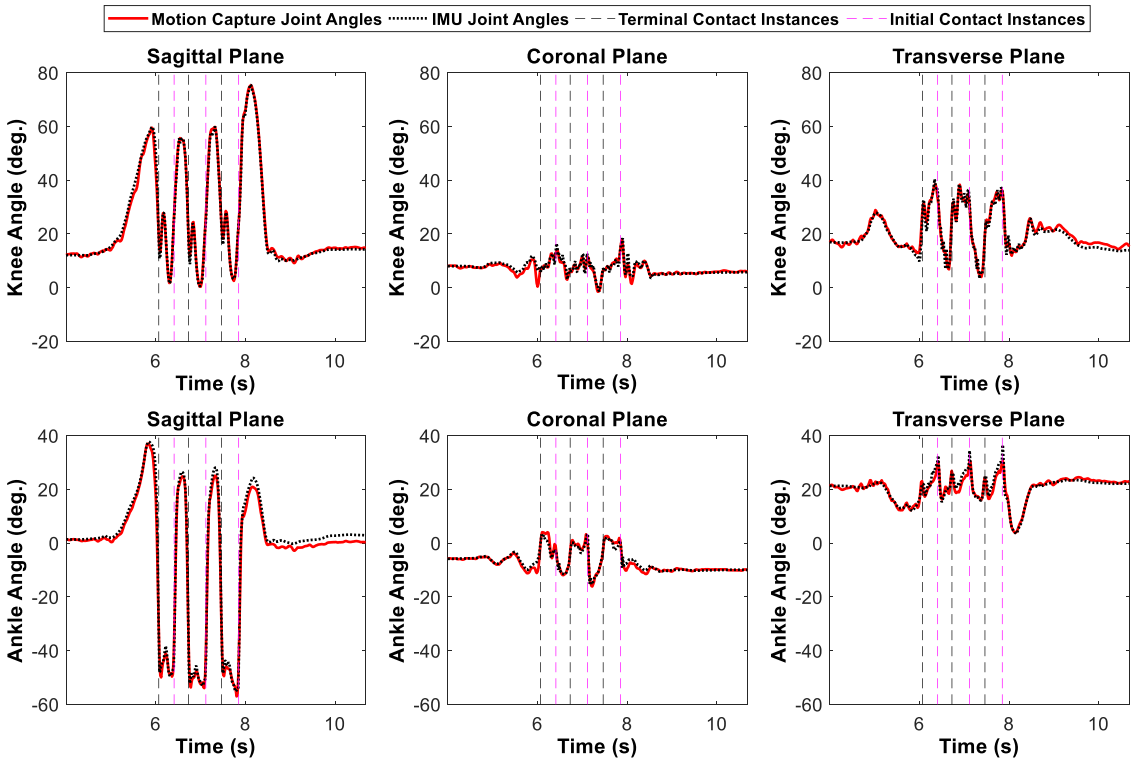

Fig. 5. The knee (upper graphs) and ankle (lower graphs) angular curves, estimated with the IMUs (dotted black curves) and with the cameras (solid red curves) in three anatomical planes for a sample TSLH trial. Hop phases are separated by vertical dashed lines.

RMS error medians (Fig. 6(a)) never exceeded 3.1 and 3.7 deg for knee and ankle in any of the anatomical planes or hop phases. ROM absolute error medians (Fig. 6(b)) were always less than 4.2 deg and 7.8 deg for knee and ankle in all the anatomical planes or hop phases. Correlation coefficient medians (Fig. 6(c)) were greater than 0.83 and 0.80 for knee and ankle in all the anatomical planes or hop phases. The angular curves within the sagittal plane, obtained by the two systems, showed the largest correlation medians of all planes, for every hop phase and both joints (>0.96 for knee and >0.91 for ankle).

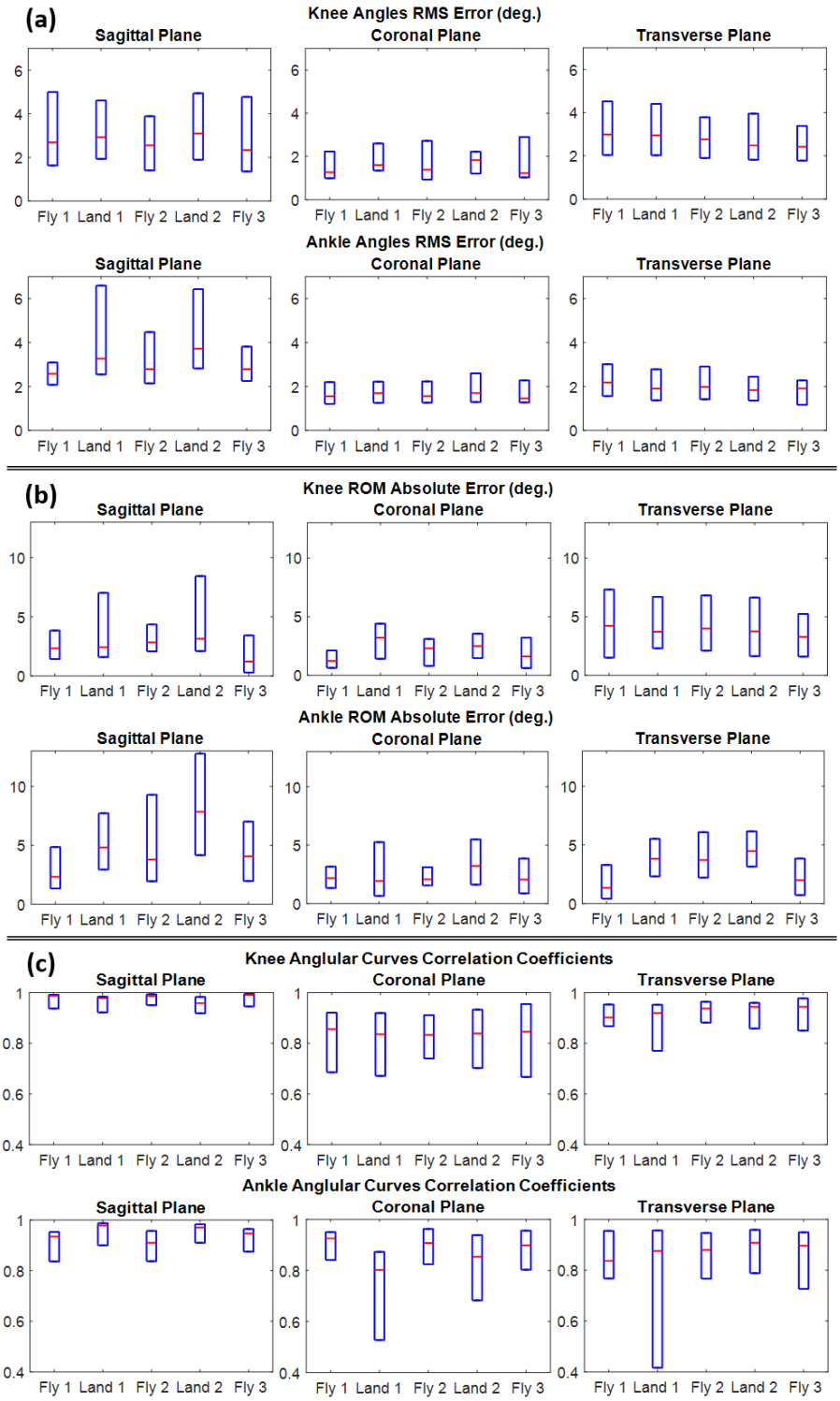

Fig. 6. Comparison of the IMU-based and camera-based knee and ankle joint angles. (a) RMS differences, (b) ROM differences, and (c) correlation coefficients between the joint angles estimated with IMUs and those obtained with cameras are presented. The results for each anatomical plane and hop phase are illustrated as box-plots among all TSLH trials of the Technical Validation study. Segments' initial orientations needed for strap-down integration are obtained with the cameras.

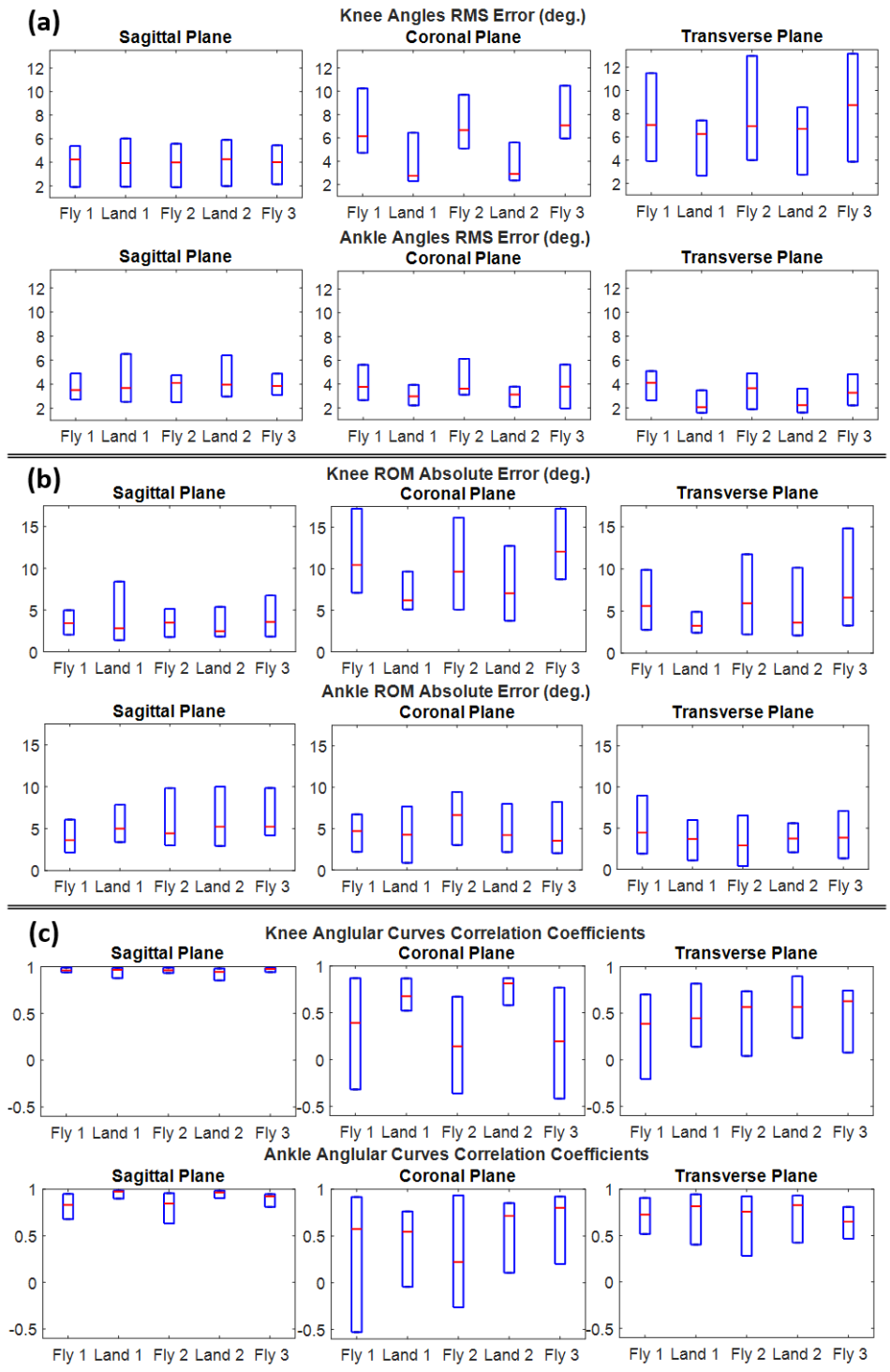

Fig. 7. Comparison of the IMU-based and camera-based knee and ankle joint angles. (a) RMS differences, (b) ROM differences, and (c) correlation coefficients between the joint angles estimated with IMUs and those obtained with cameras are presented. The results for each anatomical plane and hop phase are illustrated as box-plots among all TSLH trials of the Technical Validation study. Segments' initial orientations needed for strap-down integration are obtained based on initial tilt of the segments and assuming the heading angles to be zero.

When the segments initial orientations were estimated using IMUs, while assuming the initial heading angle of all segments to be zero, the knee and ankle angles at each hop phase were obtained with median RMS errors of less than 4.3, 7.1, and 8.8 deg in the sagittal, coronal and transverse planes, respectively, compared to the cameras (Fig. 7).

3.4.2 Clinical Research Application Results

There was no significant difference in weight and height between study groups (demographics in Table 2), however, the age of G_{UI} was significantly greater than G_I (p=0.007).

Table 3. The range of motion (ROM) of the knee and ankle joints in the sagittal plane during all the hop phases for leg sub-groups of injured and uninjured participants of Clinical Research Application study, expressed as median (IQR: inter-quartile range) among each sub-group. The significant differences (p<0.05) are marked with superscript letters and bold numbers.

Specification	Phase	Uninjured Group (G_{UI})			Injured Group (G_I)	
		Both Sides	Dominant	Non-Dominant	Injured	Non-Injured
Ankle ROM	Fly 1	21.4 (15.1)	24.7 (15.3)	20.0 (15.0)	20.9 (13.6)	23.8 (10.5)
	Land 1	**49.9 (7.3)[(a)]**	**49.0 (3.7)[(a)]**	53.0 (8.0)	52.9 (15.0)	**53.7 (7.1)[(a)]**
	Fly 2	19.2 (8.5)	18.4 (5.7)	20.7 (10.4)	20.6 (7.7)	23.1 (8.0)
	Land 2	56.1 (6.8)	56.0 (9.1)	56.1 (3.1)	57.5 (10.0)	57.8 (11.6)
	Fly 3	20.5 (12.5)	**21.4 (9.7)[(b)]**	**18.5 (12.8)[(b)]**	**23.4 (8.3)[(c)]**	**25.8 (10.9)[(c)]**
Knee ROM	Fly 1	26.2 (6.6)	25.3 (11.2)	26.6 (6.4)	25.8 (7.2)	26.9 (9.1)
	Land 1	34.5 (10.9)	**38.9 (11.6)[(b)]**	**32.4 (12.6)[(b)]**	39.1 (11.0)	37.2 (9.8)
	Fly 2	30.1 (7.0)	30.1 (8.8)	29.5 (11.8)	27.1 (5.6)	27.8 (13.8)
	Land 2	40.0 (4.7)	**40.5 (9.9)[(b)]**	**39.5 (4.9)[(b)]**	39.6 (10.2)	40.6 (8.2)
	Fly 3	**36.4 (11.5)[(d)]**	**33.3 (8.6)[(b)]**	**40.4 (8.9)[(a)(b)(d)]**	**30.8 (10.4)[(d)]**	**33.7 (8.3)[(a)]**

(a) Significant difference in joint ROMs of Non-Injured side of G_I versus Both Sides of G_{UI}, Dominant side of G_{UI}, and Non-Dominant side of G_{UI} (Non-paired comparisons)

(b) Side-to-side significant difference in joint ROMs of Dominant side of G_{UI} versus Non-Dominant side of G_{UI} (Paired comparisons)

(c) Side-to-side significant difference in joint ROMs of Injured side of G_I versus Non-Injured side of G_I (Paired comparisons)

(d) Significant difference in joint ROMs of Injured side of G_I versus Both Sides of G_{UI}, and Non-Dominant side of G_{UI} (Non-paired comparisons)

Among G_I, ankle ROM of the injured side was smaller (p=0.008) than that of the non-injured side during the third fly (Table 3). The injured leg of G_I had smaller (p=0.009) knee ROM than G_{UI} (ROMs of both sides included) during the third fly. The non-injured leg of G_I had greater (p=0.030) ankle ROM compared to the dominant side of G_{UI} during the first landing. Non-injured leg of G_I also had smaller (p=0.033) knee ROM compared to the non-dominant side of G_{UI} during the third fly. Injured/non-injured LSI (Table 4) for knee ROM was smaller (p=0.017) than the non-dominant/dominant LSI of G_{UI} during the third flying phase. Appendix B summarizes p-values of all joints' ROM and LSI comparisons conducted in Clinical Research Application study.

Table 4. Limb symmetry indices (LSIs) of range of motion (ROM) for the knee and ankle joints in the sagittal plane, during all the hop phases for leg pairs of injured and uninjured participants of Clinical Research Application study, expressed as median (IQR: inter-quartile range) among the group. The significant difference (p<0.05) in LSIs is marked with superscript letters and bold numbers.

Specification	Phase	LSI (%)	
		Uninjured Group (G_{UI}) Non-Dominant/Dominant	**Injured Group (G_I) Injured/Non-Injured**
Ankle ROM	**Fly 1**	92.0 (26.0)	88.8 (23.4)
	Land 1	104.9 (21.7)	99.1 (18.2)
	Fly 2	110.6 (51.8)	91.1 (38.3)
	Land 2	95.9 (12.1)	98.3 (17.0)
	Fly 3	82.7 (28.4)	83.2 (31.4)
Knee ROM	**Fly 1**	110.4 (30.6)	95.9 (35.3)
	Land 1	92.4 (20.7)	95.0 (24.5)
	Fly 2	114.2 (35.9)	94.7 (31.8)
	Land 2	92.3 (18.9)	92.3 (19.7)
	Fly 3	**111.3 (21.9) [(a)]**	**91.8 (34.2) [(a)]**

[(a)] Significant difference between the LSIs in ROMs of G_I and G_{UI} (Non-paired comparisons)

LSIs (in percentage) were calculated as the ratio of knee and ankle ROMs of injured (or non-dominant) leg of the participant over their non-injured (or dominant) knee and ankle ROMs.

3.5 Discussion

To the best of knowledge, this is the first study to develop an algorithm and measurement procedure for obtaining knee and ankle 3D joint angles during the TSLH using IMUs and validate the results against a reference system of motion-capture cameras. Additionally, it introduced a novel tool for lower limb joint angular measurements, compatible with clinical research conditions

and inherent simplicity of the functional tests. Such a system can be used to study fatigue, joint coordination, and variability during the challenging TSLH test. To the authors' knowledge, this is the first time that IMUs have been used for a sample of uninjured and injured participants with a recent knee injury, while performing any types of jumping tests in a clinical research setting.

The proposed IMU-based system estimated the knee and ankle 3D angles at each hop phase with median RMS errors of less than 3 deg in the coronal plane and less than 4 deg in the sagittal and transverse planes compared to the cameras. Correlation coefficients of the estimated and reference angular curves were between 0.8 and 0.99 for all the hop phases, joints, and planes. In general, the joint angle errors tended to be larger during landing phases compared to flying phases (Fig. 6). This might be due to the impact sensed by the IMUs at the time of foot-ground contact, and the resultant vibrations appearing in the IMU's signals. This is particularly evident in the small correlation coefficient obtained in the first landing phase for the 3D ankle angles (Fig 6(c)). When compared to similar studies for vertical jumping tests, our results were more accurate compared to those presented in [30] and [31] for knee angles in the sagittal plane. Notably, IMUs are expected to have more erroneous estimations of joint angles during hopping and jumping compared to walking [22,56] due to faster and jerkier lower limb motions of hopping.

The strap-down integration method needs the initial orientation of each segment to calculate the orientation in the next time frames [23]. Estimating the initial orientation without the cameras incorporation only slightly increased the errors of knee and ankle angles in the sagittal plane (maximum increase of 2.4 and 1.3 deg in median ROM error of knee and ankle at each hop phase, respectively) but resulted in notably poorer joint angle estimations in other planes (Fig. 7). While using appropriate functional calibration methods can enhance the results in the coronal and transverse planes, clinical joint angle estimations in these planes should be performed cautiously. In this study, we have only focused on joint angular differences of G_I and G_{UI} groups in the sagittal plane where the errors added by initial orientation estimation using IMUs were negligible. Additionally, for the short TSLH tests, only gyroscope drifts of the quiet standing interval at the beginning of each trial were removed to prevent error propagation along the test. Unlike walking trials [24], elimination of the gyroscope drifts was not required for every hop cycle. The high accuracy and small drift in the observed 3D joint angles (Fig. 6) indicated that the strap-down

integration of the gyroscope readouts would estimate accurate knee and ankle angles during TSLH test.

Our results indicated a tendency for smaller knee and ankle ROM of the injured side compared to the non-injured side among G_I, and were consistent with previous studies that measured knee and ankle ROM during horizontal hop tests with a camera-based system [16,19,20]. The observed modification in the kinematics of hopping might be associated with increased joints' stiffness to preserve the knee stability of the injured leg prior to and during the landing [19,21]. However, the long-term effects of these modifications and if they existed before the injury should be studied. Additionally, the reduced knee and increased ankle ROM of the injured leg of G_I compared to G_{UI} were also observed in [70] and may suggest adoption of a compensatory mechanism to overcome the knee deficits. However, the obtained joint ROMs should be further investigated by clinical experts to ensure that the reported statistically significant differences are also clinically meaningful. The lower LSI values for the knee ROM of G_I compared to G_{UI} further highlights the modifications in the kinematics of hopping between injured and uninjured groups. Nevertheless, the inter-participant variability of the LSIs, particularly for G_{UI}, indicates the need for further investigations in the future. Particularly, where the joints median ROM errors assessed in the Technical Validation study were greater than the differences between ROM medians of the leg groups in Clinical Research Application study; results should be cautiously interpreted, in accordance to the studies that have compared joint angles of the injured and uninjured leg groups with a motion-capture system.

The IMUs used in the Clinical Research Application study were a newer generation than those used in the Technical Validation. Therefore, we expected similar results from both generations of the IMUs, except that the gyroscope readouts of the newer generation would have smaller drift compared to the older one and would lead to more accurate joint angle measurements. Additionally, since our Technical Validation study mainly aimed to evaluate the efficacy of strap-down integration of gyroscope readout during TSLH test, we used the camera-based sensor-segment calibration in this study. As such, our Technical Validation study did not investigate the errors originated by functional sensor-segment calibration. However, the errors of our adopted functional sensor-segment calibration (based on quiet standing and hip flexion/extension) were

assessed in our other study [58] and were less or comparable with those reported in the literature [22,60].

We showed IMUs' potential for knee and ankle joint angle measurement during TSLH, toward developing instrumented functional tests, by evaluating the joint angles' accuracy and their ability to highlight biomechanical differences of injured and uninjured participants. Nevertheless, because the size of our convenience sub-sample was limited, age difference between G_I and G_{UI} was significant, and participants had considerable variety in their level of injuries, results of this study need more investigations to be generalized for outcome evaluation of clinical populations. Similar studies [19,20] suggest that a larger homogenous population with more severe injuries (e.g., ACL tear) would show more significant differences in joint angular usage of injured and uninjured participants during the hop tests. In the future, the reliability (reproducibility) of the IMU outcomes should also be assessed to confirm its suitability for clinical research investigations.

3.6 Conclusions

We introduced a system of 3 IMUs, fixed on the lower limb to measure 3D knee and ankle joint angles during TSLH test with high accuracy. This wearable system could identify differences in the hopping biomechanics of injured and uninjured groups in a clinical research setting and can become a powerful tool for clinicians to monitor changes in lower limbs kinematics, after knee injuries or along the rehabilitation programs. Effects of fatigue, joint synergies, and compensatory mechanisms on joint angular patterns can be quantified later to study the risks of injury/reinjury or gradual degenerative joint diseases for people with and without knee injuries.

Chapter 4

4 Quantification of TSLH Test Temporospatial Parameters with IMUs

The material covered in this chapter has been submitted as a research paper to the *Journal of Biomechanical Engineering*. The content of this chapter majorly remained identical with the submitted paper, while text formatting was conducted to fulfill the thesis requirements of University of Alberta.

N. Ahmadian, M. Nazarahari, J. L. Whittaker, and H. Rouhani, "Quantification of Triple Single-Leg Hop Test Temporospatial Parameters: A Validated Method using Body-Worn Sensors for Functionality Evaluations after Knee Injury", submitted to *Journal of Biomechanical Engineering*

4.1 Abstract

High rates of unsuccessful return to sport and early-onset osteoarthritis associated with severe sport-related knee injuries can have substantial impacts on an athlete's life. Limb symmetry index (LSI) of total distance in horizontal hop tests is commonly used by clinicians to assess deficits following sport-related injuries, while detailed temporospatial measurements typically require sophisticated force platforms and motion-capture systems. By applying an alternative measurement system of two inertial measurement units (IMUs) per limb, this study aimed to obtain flying/landing times and hop distances during the triple single-leg hop (TSLH) test, validate the results against motion-capture cameras, and assess the temporospatial parameters among injured and uninjured groups and their association with the Knee Injury and Osteoarthritis Outcome Score (KOOS). Using kinematic features of IMU recordings, strap-down integration, and velocity correction techniques, temporospatial parameters were measured for 10 able-bodied participants with median (inter-quartile range) of errors less than 10(16) ms compared to reference system for flying/landing times, and less than 4.4(5.6)% and 2.4(3.0)% of reference values for individual hops and total TSLH progression, respectively. Comparison of these parameters and corresponding LSIs

between 22 youth with sport-related intra-articular knee injuries and 10 uninjured youth highlighted the trend of differences in hopping biomechanics of these groups. For injured participants, second flying time and all hop distances demonstrated moderate to strong correlations with KOOS Symptom and Function in Daily Living subscale scores (r>0.4 except for third hop distance). These findings suggest that the IMU measurement system can successfully estimate meaningful detailed temporospatial parameters during the horizontal hop tests.

Keywords: Clinical knee assessment, Inertial measurement unit, Ambulatory monitoring, Criterion-related validation, Construct validation, Functional test

4.2 Introduction

Sport-related knee injuries, such as anterior cruciate ligament (ACL) tears, can have a significant impact on an athlete's life. In the short-term these injuries can lead to missed sport participation, reduced muscle strength, and increased risk of re-injury, while in the long-term they are associated with increased adiposity, cartilage morbidity, and premature radiographic osteoarthritis [7,9,65]. Approximately 35% of athletes fail to resume previous levels of activity two years after an ACL reconstruction, and this number grows to 50% at five years post-surgery [9,10]. According to Xergia et al. [16,17], kinematic and kinetic deficiencies of the lower limbs may continue even after return to sport (RTS) and symmetrical restoration of muscular strength. These deficiencies can alter knee joint loading, which is associated with early radiographic knee osteoarthritis and cartilage degeneration [65,71]. Close monitoring of lower limb biomechanics during functional activities can assist clinical decision making related to RTS and prevention of osteoarthritis.

Functional tests, such as vertical and horizontal bilateral or unilateral jumping tests, demand appropriate muscle strength, neuromuscular coordination, and dynamic joint stability which deteriorate with a knee injury [12,14,16]. The triple single-leg hop (TSLH) test requires controlled and consecutive unilateral hops to move the body center of mass in horizontal and vertical directions without pauses and simulates functional challenges consistent with sports maneuvers. The Limb Symmetry Index (LSI) in distance covered during horizontal hop tests is commonly used to inform RTS and rehabilitation program progression, [70] and is defined as the ratio of distance hopped on the injured leg to the distance hopped on the uninjured leg, expressed as a percentage. In contrast, for timed hop tests, the inverse of this ratio is used to define LSI based on

the time required to complete the task [7]. Commonly, an LSI cut-off value of 85% [13,21,45] is used as a milestone for RTS clearance. Despite this standard, it is important to highlight that symmetry in total hop time or distance does not guarantee unimpaired or symmetrical hopping biomechanics [40,46].

Temporospatial parameters of functional tests have been extensively assessed in laboratories using motion-capture cameras, force platforms, and contact mattresses [19,35] to better understand the consequences of knee injuries. These assessments are not feasible in clinical environments, given the sophisticated equipment, specialized operators, and time-consuming calibration, preparation, and data post-processing required. Inertial measurement units (IMUs) have been used to obtain stride length [24,62,63] and temporal events of gait [25–27,72] with relatively high accuracy and precision for injured and uninjured participants. Recently, the IMUs have also been recognized as promising tools for temporospatial analyses of various vertical jumping tests [30,32,33]. These studies used kinematic features of IMU signals for temporal estimations, and obtained the jump height based on ballistic equations, which were proposed merely for vertical jumping. To the best of our knowledge, IMUs have not been used to detect temporal events or measure forward progression during horizontal hop tests.

Therefore, in this study we explored whether a wearable system of IMUs can estimate the TSLH temporospatial parameters with sufficient accuracy and precision to highlight the trend of kinematic differences between injured and uninjured leg groups during a TSLH test. Furthermore, it was explored whether the estimated temporospatial parameters are associated with clinically relevant patient-reported outcome scores. To these ends, a wearable system of two IMUs per limb is presented in this exploratory study to estimate foot-ground Initial Contact (IC) instants and foot-ground Terminal Contact (TC) instants, calculate flying/landing times and estimate foot forward progression during TSLH test. First, the criterion-related validity of these IMU-based temporospatial parameters was assessed against reference values obtained with motion-capture cameras in Technical Validation study. Second, the construct validity of these parameters was assessed in Clinical Research Application study for a convenience sample of youth who had suffered a sport-related intra-articular knee injury and uninjured active youth to explore the injury effects on hopping kinematics. Intra-participant (side-to-side) and inter-participant (injured versus uninjured group) comparisons of temporospatial parameters, and corresponding LSIs, were

conducted among the study groups. IMU-based estimates of total TSLH progression and LSI of the injured and uninjured youth were further validated with the results obtained with a measuring tape (clinical standard). Finally, Spearman's correlation was used to assess the relationship between temporospatial parameters and KOOS subscales scores of injured participants.

4.3 Materials and Methods

4.3.1 Wearable Measurement System

4.3.1.1 Technical Validation Hardware

Two IMU modules (Physilog BFSr-3, Gait Up, Switzerland, weight: 36 g) were affixed with double-sided hypoallergenic tape to the dominant lower extremity of participants at forefoot and upper shank regions (Fig. 8). These modules wirelessly recorded 3D acceleration (range: ± 11g) and 3D angular velocity (range: ± 1200 °/s) with the sampling frequency of 500 Hz.

Fig. 8. Illustration of the Technical Validation set-up: Anatomical (applied to bony landmarks) and technical (applied to sensors boxes) markers, as well as the two IMUs, affixed on the right foot (along the second metatarsal) and leg (medial upper shank) of the participant, are represented. Among the anatomical markers, only the second and fifth metatarsal and calcaneal tuberosity markers were used for this study. No marker was present in the Clinical Research Application study.

4.3.1.2 Clinical Research Application Hardware

Four modules of lighter, recently released IMUs (Physilog 5, Gait Up, Switzerland, weight: 11 g) were bilaterally attached with Velcro straps to the feet and shanks of participants at regions consistent with the Technical Validation study. These modules were set to record 3D acceleration (range: ± 16g) and 3D angular velocity (range: ± 2000 °/s) with the sampling frequency of 256 Hz.

4.3.2 The Reference System for Technical Validation

The positions of two sets of anatomical and technical reflective markers, tracked with 8 motion-capture cameras (Motion Analysis Corporation, USA), were used as the reference to detect temporal events and foot forward progression during TSLH trials. Anatomical markers were applied to the second and fifth metatarsal heads and calcaneal tuberosity. Three technical markers were attached to each of the IMU boxes and were used for reconstruction of anatomical markers, where they were absent. Marker positions were initially recorded at 100 Hz synchronously with the IMU recordings and up-sampled to 500 Hz for comparison with the IMU-based system.

4.3.3 Experimental Protocol

4.3.3.1 Technical Validation Experiments

Through advertising on the University of Alberta campus, ten able-bodied men with no history of severe knee injuries or musculoskeletal disease volunteered to participate in the study. With the application of both IMU-based and reference systems, the participants were asked to stand motionlessly in their natural posture for 1 minute while the cameras recorded the position of both technical and anatomical markers. To avoid marker detachment during the highly dynamic hop trials, the anatomical markers were then removed and reconstructed as virtual markers based on the technical markers of the foot-sensor. The main TSLH trials started and ended with 10-second periods of standing still, and participants were asked to perform two successful TSLH trials with their dominant leg.

4.3.3.2 Clinical Research Application Experiments

From an ongoing prospective cohort of 11-19-year-old youth, a convenience subsample of 22 participants with a sport-related knee injury (group G_I), and 10 uninjured participants (group G_{UI}) were outfitted with IMUs (See Section 4.3.1.2). Knee injury was defined as a clinical diagnosis of knee ligament, meniscal, or other intra-articular tibiofemoral or patellofemoral injury that needed both medical consultation and disruption in regular sports participation. While the G_I group had

sustained a unilateral knee injury within 15 months prior to the testing date, the G_{UI} participants had no history of lower limb injuries. Prior to the testing, participants' age, bare feet standing height and weight, and dominant leg (preferred kicking leg) were recorded and participants completed the English version of KOOS questionnaire. The KOOS is a self-report measure designed to evaluate symptoms and function related to knee injury and osteoarthritis in young active patients. It consists of 42 items in five subscales (Symptom, Pain, Function in Daily Living (ADL), Function in Sports and Recreation (Sport/Rec), and Knee Related Quality of Life (QoL)) which are scored on a 5-point Likert scale. Subscale scores are transformed to a 0-100 scale with higher scores indicating better function [73].

The eligibility of participants to perform TSLH trials was assessed based on knee examinations conducted by an experienced physiotherapist and participants' KOOS scores. Only participants with a full range of knee motion and without knee effusion, or pain and difficulty during twisting/pivoting/jumping bilaterally, performed TSLH trials. Eligible participants performed two successful TSLH trials with each leg, initiated and ending with 5-seconds of upright motionless posture. A successful TSLH trial was defined as a trial in which the three hops were performed consecutively with a controlled landing after the last hop in which no extra hops or considerable ankle twists were involved. For each successful TSLH trial, the total forward progression was recorded with a measuring tape [14].

The ethics board of University of Alberta approved both parts of the study (Pro00065804 and Pro00063773), and the participants and/or their guardian provided informed written consent and/or assent prior to participation.

4.3.4 Temporal Events Detection

4.3.4.1 Reference Temporal Events

Unlike gait, where heel-strike precedes toe-strike, in TSLH, the initial contact (IC) and terminal contact (TC) can happen with any foot region. Therefore, all anatomical foot markers were reconstructed as virtual markers during the TSLH trials, assuming that the foot moves as a rigid body. The average height of each reconstructed marker during the starting motionless periods was considered as a reference level. Time frames of intersections between the recorded marker heights and their corresponding reference levels were defined as IC and TC events. Due to abrupt changes of marker heights close to IC instants resulting from sensor wobbling at the time of foot-

ground impact, the IC detection method was further refined by shifting the previously detected approximate ICs forward, to the next minimum of marker height recordings.

4.3.4.2 IMU-based Temporal Events

Peak detection algorithms for foot and shank angular velocity and acceleration signals were introduced similar to [25–27] and compared to the reference temporal instants. Methods provided by [26,27] for gait temporal events detection were modified and adapted to hopping kinematics. Likewise, all gait temporal features investigated by [25] were assessed for recordings of both foot and shank IMUs, during TSLH. Additionally, due to their relevance to hopping events and their independence to the IMUs orientation on the foot or shank, the absolute values of time-derivative of acceleration norm signal for foot and shank ($|\|A_F\|'|$ and $|\|A_S\|'|$) were assessed.

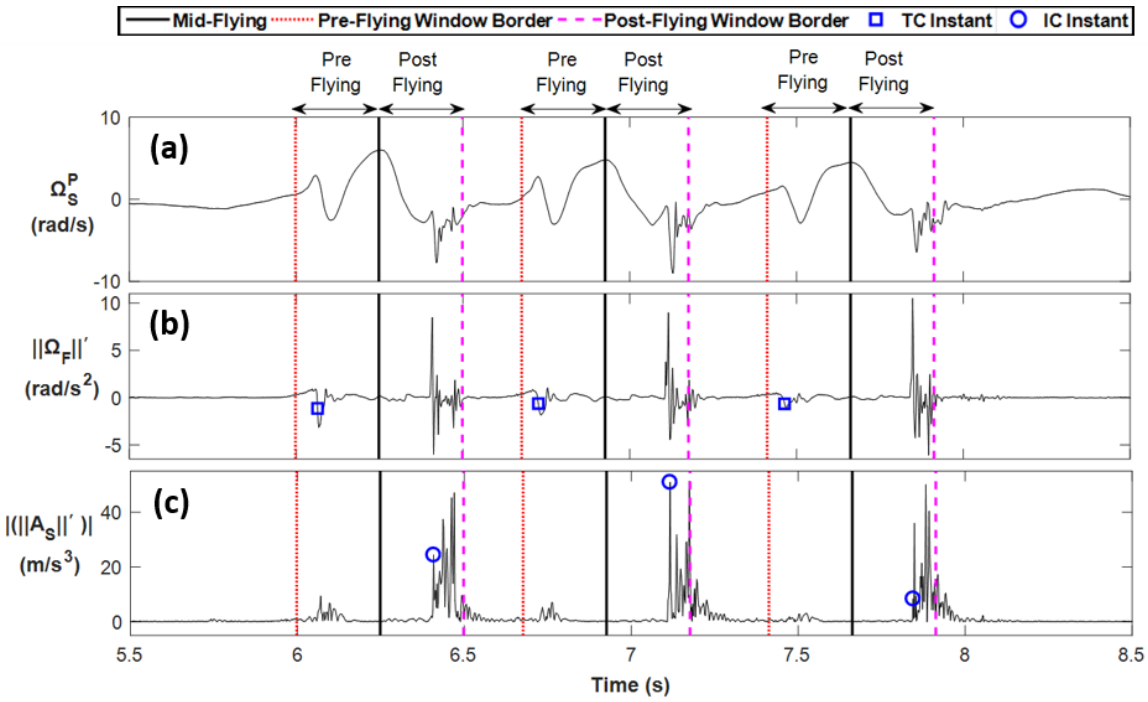

Fig. 9. TC and IC instants of a typical TSLH trial, detected using IMUs. (a): Mid-flying instants (solid vertical lines) are estimated based on shank pitch angular velocity signal (Ω_S^P). Pre-flying (dotted vertical lines) and post-flying (dashed vertical lines) phases are defined 250 ms prior and after the mid-flying instants, respectively. (b): TC instants (shown with squares) are marked on the time-derivative of foot angular velocity norm time-series ($\|\Omega_F\|'$). (c): IC instants (shown with circles) are marked on the absolute value of time-derivative of shank acceleration norm time-series ($|\|A_S\|'|$).

The global peak of shank pitch angular velocity (Ω_S^P) at each hop cycle was used as a robust feature to detect mid-flying instants [25,26] and to split each hop cycle into pre-flying and post-flying time windows for TC and IC detection (Fig. 9). We found the best IC-related feature to be

the first peak of $|\|A_S\|'|$, having an amplitude greater than 7 m/s^3 and occurring no later than 250 ms after the mid-flying instant of each hop cycle. Searching the pre-flying window of length 250 ms, we found the best TC-related feature based on the time-derivative of foot angular velocity norm, ($\|\Omega_F\|'$), at the time when its amplitude falls below -0.6 rad/s^2.

4.3.5 Forward Progression Estimation

4.3.5.1 Reference Forward Progression

The average trajectory of the foot IMU markers was considered representative of the foot trajectory. Forward progression at each hop cycle was defined as the foot frontal progression between mqs_{n-1} and mqs_n, where mqs_n marks the middle of quasi-stance phase after the n^{th} hop cycle. The quasi-stance phases were considered as the largest interval between ICs and the next consecutive TCs, where the norm of the foot angular velocity was always less than 4 rad/s.

4.3.5.2 IMU-Based Forward Progression

To obtain the forward progression during TSLH, the gravity-free acceleration of the foot in the lab global frame was double integrated, and a corrective function was defined at each hop cycle to remove the foot velocity drift caused by integration [24,62]. The gravity-free foot acceleration was calculated as in Eq. (8):

$$\vec{A}(i)^{LF}_{g\_free,foot} = {R_0}^{LF}_{TF} \times \vec{g}^{TF} - R(i)^{LF}_{TF} \times \vec{A}(i)^{TF}_{raw,foot} \quad (8)$$

where $\vec{A}(i)^{LF}_{g\_free,foot}$ and $\vec{A}(i)^{TF}_{raw,foot}$ denote the gravity-free acceleration of foot in the lab global frame and the foot-accelerometer read-out in its technical frame at each time sample (i), respectively. ${R_0}^{LF}_{TF}$ represents the rotation matrix between the foot-sensor technical frame and the lab global frame during the static stance period prior to the hopping and can be calculated based on the position of foot-sensor technical markers. In the Clinical Research Application study where the markers were not present, ${R_0}^{LF}_{TF}$ was obtained using the accelerometer readout. $\vec{g}^{TF}$ shows the median of foot-sensor acceleration readout during the static stance, with the assumption that it is caused solely by gravity. $R(i)^{LF}_{TF}$ denotes the rotation matrix between the foot-sensor technical frame and the lab global frame at each time sample, (i), and is calculated based on the strap-down integration of de-drifted foot angular velocity signal, as described in [23,24,62].

A corrective p-chip interpolation function was subtracted from the forward component of trapezoidal integration of $\vec{A}(i)^{LF}_{g\_free,foot}$ to derive foot forward velocity. This corrective function was defined over $[mqs_{n-1}, mqs_n]$, with the axillary point aqs_n at 75% of this interval, as in Eq. (9):

$$f_c\,(n) := pchip\big(\{mqs_{n-1}, aqs_n, mqs_n\}, \{V_F(mqs_{n-1}), min\big(V_F(mqs_{n-1}), V_F(mqs_n)\big), V_F(mqs_n)\}\big) \quad (9)$$

where $f_c(n)$ and V_F denote the defined corrective function and the non-corrected foot forward velocity, respectively (Fig. 10). Finally, foot forward progression was derived from the integration of corrected foot forward velocity.

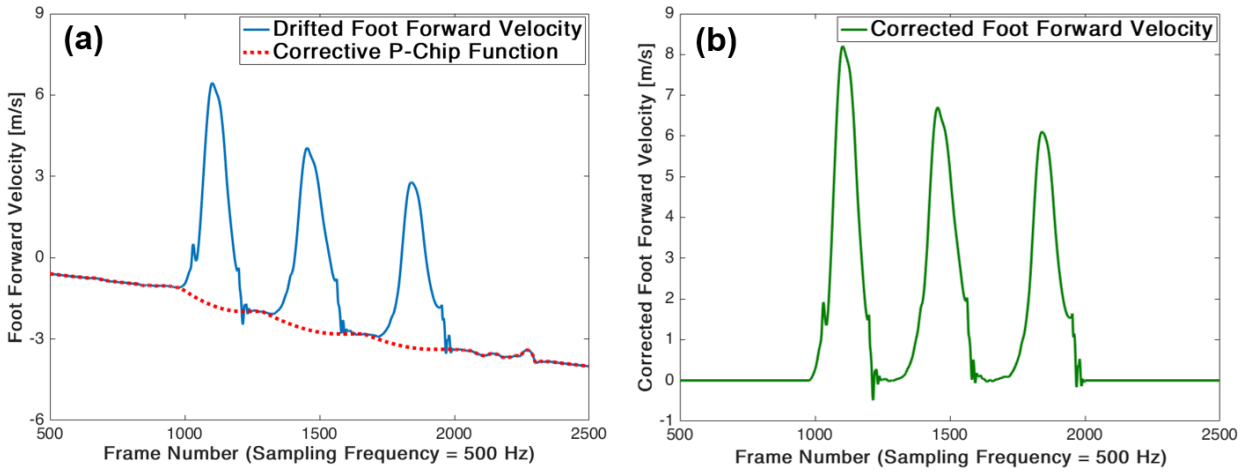

Fig. 10. Removing the drift of foot forward velocity, caused by trapezoidal integration of foot forward acceleration, for a sample TSLH trial. (a): The drifted foot forward velocity (blue solid curve) and corrective p-chip function (red dotted curve) are shown. (b): The corrected foot forward velocity (green solid curve) has been obtained by subtracting the corrective p-chip function from the drifted foot forward velocity.

4.3.6 Data Analysis

In Technical Validation study, 60 hop cycles (10 participants × 2 trials × 3 hops at each trial) were investigated, and the temporospatial parameters obtained by IMUs were compared to those obtained by the reference system. In Clinical Research Application study, 132 hop cycles (22 participants × 2 trials × 3 hops) and 60 hop cycles (10 participants × 2 trials × 3 hops) were investigated for each leg of G_I and G_{UI}, respectively. For all participants, three hopping forward distances, total TSLH forward progression, three flying and two landing times, and corresponding LSIs were calculated based on IMU signals. The averaged temporospatial parameters over the two trials recorded from each leg, were considered for statistical analysis. As the normality of the

samples was rejected for a number of investigated parameters using Jarque-Bera test, Wilcoxon signed-rank test and Wilcoxon rank-sum test were used for intra-participant (side-to-side) and inter-participant (injured/uninjured legs of G_I compared to dominant/non-dominant/both legs of G_{UI}) comparisons, respectively. Multiple comparisons were not used, as each of the temporospatial parameters was targeted as a potential TSLH outcome and the purpose of comparisons was not to make clinical conclusions. Clinical relevance of the obtained temporospatial parameters and LSIs was further explored by calculating their Spearman's correlation with G_I's KOOS subscale scores.

4.4 Results

4.4.1 Estimations of Temporospatial Parameters: IMU versus Reference Systems

Characteristics of the participants who enrolled in Technical Validation and Clinical Research Application studies are shown in Table 5.

Table 5. Characteristics of the participants enrolled in the Technical Validation and Clinical Research Application studies. For the participants of Clinical Research Application study, self-reported KOOS scores are also presented.

Characteristics	Technical Validation (n=10)		Clinical Research Application (n=32)	
	Injured (n=0)	Uninjured (n=10)	Injured† (n=22)	Uninjured† (n=10)
Sex (W/M)	-	0W/10M	17W/5M	9W/1M
Age* (years)	-	23 ± 3	16 ± 1	17 ± 2
Height* (cm)	-	177 ± 10	167 ± 12	171 ± 9
Weight* (kg)	-	68 ± 8	60 ± 14	65 ± 10
Dominant Leg (R/L)	-	10R/0L	19R/3L	10R/0L
Injured Leg (R/L)	-	-	12R/10L	-
Injured Leg (D/ND)	-	-	11D/11ND	-
KOOS Symptom*	-	-	84 ± 16	95 ± 6
KOOS ADL*	-	-	99 ± 4	100 ± 0
KOOS Pain*	-	-	90 ± 14	100 ± 0
KOOS Sport/Rec*	-	-	85 ± 20	100 ± 0
KOOS QoL*	-	-	50 ± 30	100 ± 5

n: Number of participants; W: Woman; M: Man; R: Right; L: Left; D: Dominant side; ND: Non-dominant side

ADL: KOOS subscale for Function in Daily Living, Sport/Rec: KOOS subscale for Function in Sports and Recreation, QoL: KOOS subscale for Knee Related Quality of Life

†Injured and uninjured groups of participants of the Clinical Research Application study are referred to as G_I and G_{UI}, respectively, within the body of this chapter.

*Age, height, weight, and self-reported KOOS scores are presented as median ± interquartile range among the participants.

For Technical Validation trials, the proposed kinematic features of IMU signals estimated the IC and TC instants with median (inter-quartile range: IQR) errors of 2(20.5) and 11(22.5) ms, respectively, compared to the reference system. These errors in IC and TC detection were equal to 0(2) and 1(2) time sample of the reference system recordings, respectively. Flying (60 flying phases) and landing (40 landing phases) times were estimated with median (IQR) differences of -4(18) and 5(16.5) ms from the reference values (i.e., 0(2) and 1(2) time sample of the reference system recordings). Individual hop distances (60 hops) were estimated with 4.4%(5.6%) relative error while the total TSLH progression (20 TSLH trials) were estimated with 2.4%(3.0%) relative error compared to the reference system (Table 6). In Clinical Research Application study, comparison of the IMU-based total TSLH forward progression with the values obtained with a measuring tape showed median (IQR) relative errors of 2.9%(3.5%) and 3.2%(2.9%) (LSIs absolute errors of 4.8%(3.0%) and 3.9%(2.1%)) for G_I and G_{UI}, respectively.

Table 6. Errors of the proposed IMU system in the estimation of temporospatial parameters of TSLH against the motion-capture system. Results are expressed as 25%, 50% and 75% percentiles of error, calculated for all 60 individual hops (20 TSLH trials, 3 hops each) performed by the 10 able-bodied participants. The values in parentheses for the temporal parameters express the errors in terms of time sample of the motion-capture system (10 ms).

Validated Parameter	**Error**					
	[25%	**50%**	**75%]**	**[25%**	**50%**	**75%]**
Temporal Parameters	**Error (ms & sample)**			**Absolute Value of Error (ms & sample)**		
Initial Contact Instants	[-9(-1)	2(0)	12(1)]	[4(0)	12(1)	20(2)]
Terminal Contact Instants	[-7(-1)	11(1)	16(2)]	[10(1)	14(1)	20(2)]
Flying Times	[-12(-1)	-4(0)	6(1)]	[5(1)	10(1)	18(2)]
Landing Times	[-3(0)	5(1)	14(1)]	[4(0)	10(1)	20(2)]
Forward Progression Distances	**Relative Error (%)**			**Absolute Error (cm)**		
First Hops	[3.62	5.50	6.31]	[4.46	6.11	7.17]
Second Hops	[1.71	3.05	6.52]	[1.90	3.82	7.54]
Third Hops	[2.15	5.64	8.65]	[2.39	7.39	10.78]
All Individual Hops	[2.08	4.44	7.69]	[2.42	5.41	9.77]
Total TSLH Progression	[1.03	2.40	4.01]	[3.83	9.35	14.12]

4.4.2 Comparison of Temporospatial Results among Injured and Uninjured Youth

No significant difference was observed for the height and weight between study groups (see Table 5 for participant characteristics); however, G_I was significantly younger than G_{UI} (p=0.007).

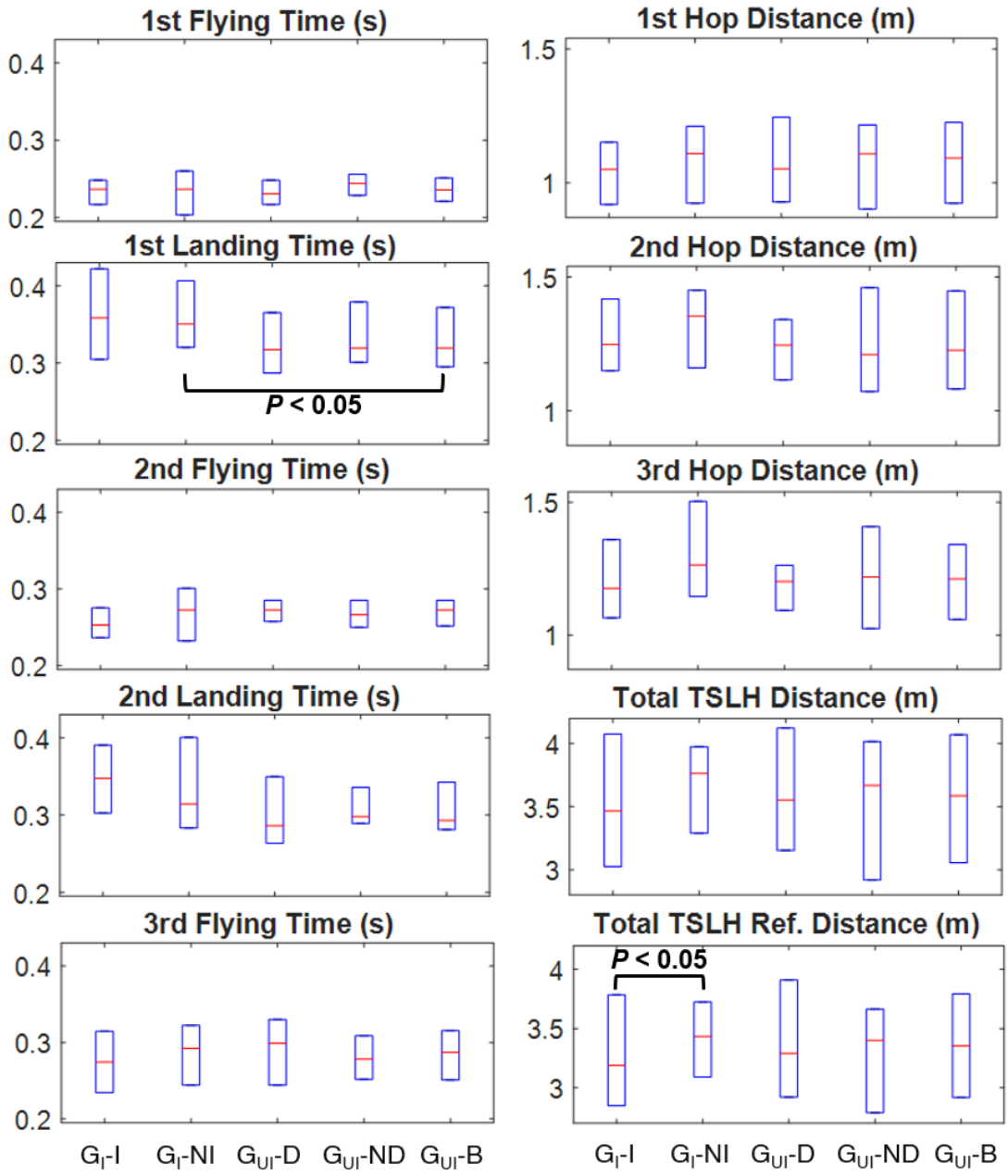

Fig. 11. Comparison of temporospatial parameters among all different leg sub-groups of injured (G_I) and uninjured (G_{UI}) participants. Temporospatial parameters were estimated with IMUs or measured with a measuring tape (shown as Total TSLH Ref. Distance). Box-plots on the left and right sides represent time- and distance-related parameters, respectively. (Leg sub-groups are shown with G_I-I: G_I's Injured Leg, G_I-NI: G_I's Non-Injured Leg, G_{UI}-D: G_{UI}'s Dominant Leg, G_{UI}-ND: G_{UI}'s Non-Dominant Leg and G_{UI}-B: G_{UI}'s Both Legs.)

No significant differences (α=0.05) were observed in any of the inter- and intra-participant comparisons of IMU-based temporospatial parameters and LSIs, except for the first landing time (p=0.049 between the non-injured side of G_I and both sides of G_{UI}). Appendix C summarizes p-values of all temporospatial and LSI comparisons conducted in Clinical Research Application study. Total TSLH progression measured with a measuring tape showed a significant difference (p=0.028) for the intra-participant comparison of the G_I. However, no other statistically significant differences were found between the compared temporospatial parameters or LSI values. Nevertheless, tendencies in differences among temporospatial parameters of leg sub-groups (injured/non-injured sides of G_I, dominant/non-dominant/both sides of G_{UI}) were observed (Fig. 11). First, the non-injured side of G_I tended to have the greatest individual and total hop distance among all the sub-groups, while the injured side tended to have the least distance except for the second hop. Second, the injured side of G_I tended to have the longest landing and shortest flying times of all sub-groups, except for the first flying. The dominant side of G_{UI} tended to have the shortest landing and longest flying times of all sub-groups, except for the first flying.

4.4.3 Correlations between KOOS and Temporospatial Parameters in Injured Youth

Based on both measuring systems (IMU and measuring tape), all individual and total hop distances of the G_I's injured side moderately correlated with the KOOS Symptom subscale score ($0.403<r<0.502$) (Table 7). All individual and total hop distances of G_I's injured side except for the third hop distance also moderately correlated with the KOOS ADL subscale score ($0.407<r<0.429$). The KOOS Symptom and ADL scores also moderately correlated with LSI values of total TSLH distance measured with tape (r=0.414) and IMU-based second hop distance LSI (r=-0.407), respectively. Among the temporal parameters, the second flying time showed strong (r=0.660) and moderate (r=0.448) correlation with the KOOS Symptom and ADL subscale scores, respectively. No moderate or strong correlation was observed between temporal LSIs and KOOS scores, except for the LSI calculated based on second flying time and KOOS Symptom score (r=-0.536). Generally, the correlations of both Symptom and ADL KOOS scores were considerably stronger with flying times rather than landing times (Table 7). Nearing the end of TSLH trials, correlations increased between the hopped distances and the Symptom subscale, while the opposite trend was observed for ADL subscale. All other KOOS subscale scores had very weak or weak correlation with the calculated temporospatial parameters and LSIs except for

a correlation between second flying time and Function in Sports and Recreation subscale score (r=0.401) and correlations of second hop distance LSI with KOOS Pain subscale (r=-0.402) and Knee Related Quality of Life subscale (r=-0.545) scores.

Table 7. Spearman's correlation coefficients between self-reported KOOS subscales and temporospatial parameters obtained with IMUs or measuring tape for the injured leg of the injured participants (G_I) during all the phases of TSLH. Significant correlations are marked with asterisks and bold numbers.

KOOS Subscale	Time					Time Asymmetry				
	Fly 1	**Land 1**	**Fly 2**	**Land 2**	**Fly 3**	**Fly 1**	**Land 1**	**Fly 2**	**Land 2**	**Fly 3**
Symptom	0.166	0.003	**0.660***	0.055	0.381	-0.117	0.049	**-0.536***	0.245	0.016
ADL	0.390	-0.027	**0.448***	0.085	0.157	-0.225	0.254	-0.366	0.291	0.044
Pain	0.126	0.052	0.253	0.095	-0.056	-0.054	-0.014	-0.148	0.082	0.317
Sport/Rec	0.117	-0.035	0.401	-0.075	0.067	-0.070	0.109	-0.363	0.357	0.108
QoL	0.001	-0.150	-0.062	-0.005	-0.158	-0.249	0.338	-0.137	0.328	-0.121
KOOS Subscale	**Distance**					**Distance Asymmetry**				
	Hop 1	**Hop 2**	**Hop 3**	**TSLH Total**	**TSLH Total (Ref.)**	**Hop 1**	**Hop 2**	**Hop 3**	**TSLH Total**	**TSLH Total (Ref.)**
Symptom	0.403	**0.485***	**0.502***	**0.494***	**0.502***	0.259	-0.201	0.312	0.177	0.414
ADL	**0.429***	0.414	0.327	0.407	**0.422***	0.178	-0.407	0.181	0.024	0.324
Pain	0.245	0.175	0.206	0.222	0.253	0.115	-0.402	0.137	-0.044	0.170
Sport/Rec	0.308	0.259	0.157	0.273	0.263	0.168	-0.363	0.087	-0.039	0.231
QoL	0.119	0.203	0.222	0.151	0.239	-0.041	-0.545	0.071	-0.156	0.059

ADL: KOOS subscale for Function in Daily Living, Sport/Rec: KOOS subscale for Function in Sports and Recreation, QoL: KOOS subscale for Knee Related Quality of Life

TSLH Total (Ref.): Reference values of total hopped distance, measured with a measuring tape

Distance-based LSIs (in percentage) were calculated as the ratio of distance that participants have hopped with their injured leg over the distance they have achieved with their non-injured leg.

Time-based LSIs (in percentage) were calculated for each hop phase as the ratio of the time that the participants needed to hop on their non-injured leg over the time that they needed to hop on their injured leg.

4.5 Discussion

In this study, IMUs were used for the first time to calculate the forward progression and flying/landing periods during each phase of TSLH test and the results were validated against a reference system of motion-capture cameras. The efficacy of the introduced temporospatial measuring system was then explored in a clinical research environment for intra-participant and inter-participant comparisons between groups of uninjured and injured youth. Such a system can

be used to break down the horizontal hop tests into their sub-phases and measure the temporospatial parameters along the multiple horizontal hops. To the authors' knowledge, it is the first time that the jumping/hopping distance during the functional tests has been calculated directly based on the acceleration of body segments rather than the flying time.

Our proposed algorithm was able to robustly detect the IC and TC instants of the TSLH tests with median errors of less than 11 ms (i.e., one time sample of the reference system recordings). As expected, the error of TC detection was slightly higher than IC, as TCs are smoother temporal events and in contrast to ICs, are not associated with abrupt changes and peaks in IMU recordings. These errors were comparable to those of [25–27] obtained for temporal parameters of gait. However, notably larger errors are expected in the detection of temporal parameters due to the jerky motion of the foot in TSLH test, accompanied by severe IMUs wobbles. Compared to vertical jumping studies [30,32], we obtained similar accuracy and precision in temporal parameters detection. However, those studies had removed the constant erroneous offsets of IC and TC estimation from their results.

The accuracy and precision of our estimated forward progression during TSLH were comparable to those reported in [24] for stride length estimation. While we estimated individual hop distances with a median error of 5.41 cm, [62] reported RMS error of about 18 cm for gait progression estimation. Additionally, as shown in Table 6, the error of forward progression estimation does not increase along the test, which was to be expected according to [55] for a short test such as TSLH (duration less than 30 seconds). Therefore, removing the gyroscopes' static drift at the beginning of the TSLH trial effectively eliminated gyroscope-based errors, and further correction for these errors was not required.

The significant correlations of IMU-based temporospatial parameters with KOOS Symptom and ADL subscales emphasized the relevance and importance of monitoring each hop in detail during the TSLH test to interpret those scores during functionally challenging activities, rather than merely recording the total distance. The validity, responsiveness, and reliability of KOOS for populations with various knee injuries have been reported by several studies [7,43,74]. Our results show that injury symptoms are highlighted toward the end of the test when the activity becomes more challenging, while knee deficiencies for ADL are highlighted at the time of activity initiation. As the IMU-based system can provide instantaneous temporospatial information during TSLH

test, the interpretation of KOOS subscale scores in association with temporospatial parameters would be feasible for clinical scientists. Furthermore, the consistent trend of correlations between temporospatial parameters and KOOS Symptom and ADL scores along the TSLH makes them more reliable for clinical interpretations.

Although no significant difference was observed for IMU-based temporospatial parameters among injured and uninjured youth (possibly due to the heterogeneity of injury, variability in time since injury, and small sample size), the proposed measuring system showed consistent results with previous studies [19,21] on shorter distances hopped on G_I's injured leg. Although the total TSLH progression measured by tape showed significant intra-participant difference for G_I (p=0.028), it is not clear how the process of eyeballing the tape numbers in clinics would affect the accuracy of this method. The proposed IMU-based system was validated with the gold standard of motion-capture with a median error of 2.4% for total TSLH progression and resulted in p=0.088 for this case, in which median LSI of total hop progression for G_I was 94.3%. It is also noteworthy that the temporospatial errors of the IMUs system (assessed in Technical Validation study) should always be considered when comparing the median temporospatial parameters between injured and uninjured leg groups to avoid misinterpretation of the results.

Note that we used a recently released generation of IMUs in Clinical Research Application study, with which we expected to obtain more accurate results than those used for Technical Validation study. Additionally, we obtained the initial orientation of the IMUs in Clinical Research Application study only based on IMUs recordings, rather than using cameras. Nevertheless, the median relative error of the estimated total hopped distance and the absolute error of its corresponding LSI were below 5% (compared to those measured by tape as a secondary reference system). This confirmed the accuracy of the IMU system used in the Clinical Research Application study, in the absence of the cameras' benefits. In the future, the reproducibility of the IMUs temporospatial outcomes should be also assessed to ensure about the reliability of the system for clinical research investigations.

The proposed IMU-based system is expected to measure temporospatial parameters accurately for similar horizontal hop tests. The development of the algorithm for 3D foot trajectory estimation can provide further details for the tests such as crossover horizontal hops, where the lateral trajectory of foot can also be of interest. Furthermore, verbally encouraging the participants to

perform consecutive hops during TSLH and rejection of trials with longer pauses between the hops might conceal the tendency to longer landing times in injured participants. These longer pauses might be due to more time that injured participants need to re-coordinate their joints for the next hop and can be a result of stiff landing strategies [16,21]. As our proposed system can accurately estimate landing times, there is no need for the further implication of such standards as "hopping without pauses", and a modified TSLH test can be introduced in which the participants hop at their comfortable pace. Therefore, enhancement and comparison of the existing hop tests will be feasible in the future, in order to introduce a test which can address knee deficits more comprehensively.

4.6 Conclusions

We presented a system of two IMUs fixed on shank and foot, capable of estimating foot-ground IC and TC instants, and forward progression along the horizontal hop tests such as TSLH, and demonstrated its accuracy and precision. This system can help clinician-scientists to study the detailed biomechanical parameters of hopping during rehabilitation programs, as relevant variables to clinically meaningful scores and decide about RTS onset with more confidence.

Chapter 5

5 Conclusion and Future Perspectives

5.1 General Results and Main Contributions

The main goals of this thesis project were to: (1) develop a methodology for detailed kinematic measurements (i.e., 3D joint angles and temporospatial parameters) during the TSLH tests using IMUs, (2) validate the IMU-based measurement system against the motion-capture system to ensure about high accuracy (small medians of errors) and precision (small inter-quartile ranges of errors) of the results, (3) assess the capabilities of the proposed wearable system in the clinical research environment to reveal kinematic differences between hopping strategies of injured and uninjured leg groups, and (4) evaluate the relevance of the obtained kinematic parameters with established patient-reported scores for symptom and function.

In order to accomplish these goals, novel algorithms for estimation of 3D angles of the knee and ankle joints, flying and landing periods, and foot forward progression with IMUs were developed, adapted, and validated for horizontal hop tests for the first time. Accurate and precise estimation of the aforementioned parameters allowed us to be the first to apply the wearable IMUs system during horizontal hop tests in a clinical research setting on groups of participants who had suffered from recent knee injuries (less than two years after injury) and uninjured participants in order to monitor the kinematics of their hops thoroughly. The obtained kinematic parameters revealed inter-participant and intra-participant differences among the injured and uninjured groups and were correlated with injured participants' self-reported scores of symptoms and difficulties in daily living function. Therefore, a novel and promising joint angular and temporospatial measurement tool for horizontal hop tests was presented, which is compatible with the inherent simplicity of the functional tests, and well-suited to be used in clinical research settings.

The proposed algorithms, which have similar concepts of temporospatial and joint angles estimation of well-known gait algorithms, were adapted to horizontal hope tests facing several

complexities. These complexities, as well as the main outcomes of our analysis, are addressed in the next sections.

5.1.1 Complexities and Outcomes of 3D Joint Angles Estimation

The higher dynamics of hopping compared to gait can be the source of many errors such as slight slippage of IMUs on the body segments, deformation of body segments, vibrations of the soft tissue on which IMUs are attached, shortened or disappeared foot-flat intervals at each hop, saturation of the range of accelerometers and gyroscopes, and increased gyroscopes' drift due the complicated and dynamic movements [29,54,55]. We attempted to avoid IMUs slippage during hopping by double securing them to the body segments with single- and double-sided hypoallergenic tapes and Velcro straps. Additionally, to minimize the impact of soft tissue vibrations, the IMUs were attached to the bony regions, and their readouts were low-pass filtered to decrease soft tissue artifacts. Despite the mentioned complexities, the proposed joint angle measurement algorithm successfully estimated 3D angles with overall (all participants, all hop phases, and all anatomical planes) median RMS error and ROM error of less than 2.3 and 3.2 deg, respectively, and correlation coefficients of above 0.92 compared to the camera-based angles for both knee and ankle. These results are more accurate than the results reported in similar vertical jumping studies [30,31] and comparable to the results of gait studies [23,28,56]. The knee and ankle ROMs are expected to be greater during hop tasks compared to gait, and this would improve the relative ROM errors of our proposed system. Consequently, the proposed wearable system identified compensatory mechanisms developed by the injured limb to reduce knee and ankle ROM during the third fly compared to an uninjured or contralateral limb (preparing for a more upright, stiffer landing) and revealed the greater asymmetry in the knee ROM of injured participants compared to uninjured participants.

The shortness of functional tests has played an important role in the prevention of large gyroscopes' drifts to affect our results. It is notable that in the proposed algorithm, strap-down integration has been applied only once from beginning to the end of each trial, and segments' tilt and heading angle were not updated at each hop cycle. The reason behind taking this approach is that, during hopping, segments experience high accelerations even during the landing periods, and updating the segments tilt based on gravity vector might further increase the errors. Furthermore, participants have less control over their foot landing during hops compared to the foot-flat phases

of gait, and assuming the segments heading angle to be zero during the landing phases of the TSLH might not be acceptable. All in all, the strap-down integration method seemed to provide accurate and stable results during the TSLH trials, as Fasel et al. [55] have mentioned for short activities (duration less than 30 seconds), while the only implemented correction was removing the static offset of gyroscopes' signals along the corresponding TSLH trial.

5.1.2 Complexities and Outcomes of Temporospatial Estimation

As mentioned in Section 4.3.4.1, during hopping, the IC and TC events can happen with any foot region and have a more general definition than heel-strike and toe-off, which happen during gait cycles. As such, it is more challenging to detect these events, because the amplitude of the peaks of acceleration and angular velocity signals which correspond to these events can considerably change based on the location of the sensor and the foot-region that touches the ground initially or leaves the ground terminally. To address this problem, all the kinematic signal features that had been proposed in the literature previously [25–27,61] for toe-off, toe-strike, heel-off and heel-strike were adapted for both foot (as the segment which is directly in contact with the ground) and shank (as the segment which is less influenced by the noise originated from foot-ground impact) IMUs. Results of all tested kinematic signal features can be found in Appendix D. With the selection of the appropriate signal features, the temporal detection median (IQR) errors were minimized to 2 (20.5) ms and 11 (22.5) ms for the IC and TC instants, respectively and were comparable to vertical jumping studies [30,32], which reported their results after removing the systematic errors of their events detection algorithms.

The estimation of frontal foot velocity depends on accurate estimation of the segments' orientations (to cancel the gravity component of accelerometers' readout) and temporal events (to find the mid-point of quasi-stance phases and set the foot frontal velocity to be zero). Accordingly, our proposed algorithms had already fulfilled the preliminary requirements for accurate foot frontal progression estimation during hopping. Therefore, the corrective p-chip function that was proposed for TSLH (inspired by Mariani's algorithm for gait [24]) removed the integration drift from foot frontal velocity and minimized the median (IQR) of errors to 5.41 (7.35) cm for individual hop distances and 9.35 (10.29) cm for total TSLH progression. Relative accuracies of our results of foot frontal progression during TSLH were 4.44% and 2.40% for individual hop distances and total TSLH progression, respectively. Comparing these numbers with the accuracy

of Dowling's estimations [30] for drop jump heights (20.20% relative error), our method of deriving the distance directly based on foot acceleration was notably more favorable than their method of defining ballistic equations to find jump height as a function of flight time. Our proposed method was also the first-ever attempt to find spatial parameters of hopping/jumping functional tests, based on the integration of accelerometer's signal.

Clinically, the proposed temporospatial estimation algorithm provides an appropriate tool for interpretation of the knee-related questionnaires such as KOOS. In our study, stronger correlation of the obtained temporospatial parameters with Symptoms scores towards the end of the TSLH could suggest that symptoms such as a swollen knee become more problematic at the end of a demanding activity such as TSLH. On the other hand, stronger correlation of the obtained temporospatial parameters with ADL scores at the beginning of TSLH could suggest that knee deficiencies that appear during daily living function also influence the initial phase of demanding activities such as TSLH. These interpretations need further investigation by clinicians and experts to be confirmed.

5.2 Future Perspectives

5.2.1 Application of IMUs for Instrumented TSLH Tests in Clinics

We cautiously avoided talking about the use of the validated novel measurement system in clinics for temporospatial and joint angles measurements during TSLH. Yet, the following features make the wearable system of IMUs a powerful option for kinematic monitoring during the horizontal hop tests: (1) low cost, (2) high accuracy and precision, (3) minimal preparation and calibration time (less than 5 minutes), (4) compatibility with simplicity of the hop tests, (5) ease of use for inexperienced operators, and (6) portability and minimal interference with performance of hop tests. For clinical use, further investigation should be performed on healthcare professionals' and patients' acceptance rate of this system, the possibility of allocating 5 minutes extra time during the clinical visits to benefit from advantages of this system, and the simplicity of using this system by the personnel who are unfamiliar with the concepts of wearable systems. During our Clinical Research Application study, no participant complained about the application of IMUs, and most of them were eager to wear IMUs for detailed monitoring of their performance. Furthermore, the research assistants who were unfamiliar with IMUs and details of the algorithms showed to be confident in using them after one training session.

5.2.2 Application of IMUs for a Battery of Instrumented Horizontal Hop Tests

The proposed algorithms in this thesis exploit the dynamics of hopping and initial posture prior to hopping in order to find TSLH kinematic parameters. Therefore, it is expected that these algorithms also have a good performance in finding kinematic parameters of other similar horizontal hop tests, such as the single-leg hop, triple crossover hop, and 6-m timed hop tests. The only restriction is that the horizontal hop test of interest should be relatively short (less than 30 seconds) so that gyroscopes' dynamic drift can be negligible. Consequently, a complete battery of horizontal hop tests can be performed in clinics, while joint angles and temporospatial parameters are being monitored. Further, by comparing the kinematics of these tests, it can be decided which of them is superior to the others, based on the challenges that these tests provide to highlight the knee deficits. Finally, an optimal standard hop test can be designed that effectively incorporates different kinematic aspects of various hop tests and simulates the real challenges that lower limb is subjected to, during sports maneuvers.

5.2.3 3D Visualization of the Hop Tasks with a Virtual Skeleton

The physiotherapists can benefit from watching the hop tasks performed multiple times from various angles, in slow motion, and directly watching the kinematic relationship between segments and joints. The proposed algorithms can be expanded to find the vertical and mediolateral trajectory of the foot during hopping. According to Mariani [24], 3D foot trajectory tracking is expected to be feasible in the same fashion that the frontal foot trajectory was calculated. The trajectory of the shank and thigh can then be obtained based on the length and orientation of these segments with respect to the foot. Accordingly, the 3D animation of the participant's virtual skeleton during hopping can be created based on orientation, trajectory, and length of the lower limb segments.

Additionally, the hip and trunk sagittal angles have been mentioned to be associated with the compensatory mechanisms that the adjacent joints develop after knee injuries to compensate for knee deficits [19,20,30,37]. Therefore, placing an IMU on each of these segments to calculate the sagittal angles can provide further information regarding the compensatory mechanisms to the physiotherapists. These segments can also be added to the aforementioned virtual skeleton representation.

5.3 Conclusions

In this project, a wearable system of IMUs was introduced for kinematic monitoring of horizontal hop tests in a clinical research setting. This system has the required accuracy and precision for estimating 3D knee and ankle angles, IC and TC instants, flying/landing times, and individual and total hop distances of the TSLH test. The kinematic outcomes of this wearable system were clinically relevant and could reveal the differences in hopping strategies between injured and uninjured leg groups. If the reliability (reproducibility) of this system is confirmed and its acceptance rate is high among patients and clinicians, it can be used for kinematic monitoring of similar hop tests in clinics and its outcomes can be provided as an animation (in the form of a virtual skeleton) to the clinicians to perform a thorough kinematic assessment.

References

[1] J.M. Billette, T. Janz, Injuries in Canada: Insights from the Canadian Community Health Survey, Stat. Canada Cat. No. 82-624-X. (2015). https://www150.statcan.gc.ca/n1/pub/82-624-x/2011001/article/11506-eng.htm (accessed September 20, 2009).

[2] J.L. Whittaker, C.M. Toomey, A. Nettel-aguirre, J.L. Jaremko, P.K. Doyle-baker, L.J. Woodhouse, C.A. Emery, Health-related Outcomes after a Youth Sport–related Knee Injury, Med. Sci. Sports Exerc. 51 (2018) 255–263. doi:10.1249/MSS.0000000000001787.

[3] R. Bahr, T. Krosshaug, Understanding injury mechanisms: A key component of preventing injuries in sport, Br. J. Sports Med. 39 (2005) 324–329. doi:10.1136/bjsm.2005.018341.

[4] S.M. Trigsted, E.G. Post, D.R. Bell, Landing mechanics during single hop for distance in females following anterior cruciate ligament reconstruction compared to healthy controls, Knee Surgery, Sport. Traumatol. Arthrosc. 25 (2017) 1395–1402. doi:10.1007/s00167-015-3658-9.

[5] E. Tengman, L. Brax Olofsson, K.G. Nilsson, Y. Tegner, L. Lundgren, C.K. Häger, Anterior cruciate ligament injury after more than 20 years: I. Physical activity level and knee function, Scand. J. Med. Sci. Sport. 24 (2014) e491–e500. doi:10.1111/sms.12212.

[6] J. Baltich, J. Whittaker, V. Von Tscharner, A. Nettel-Aguirre, B.M. Nigg, C. Emery, The impact of previous knee injury on force plate and field-based measures of balance, Clin. Biomech. 30 (2015) 832–838. doi:10.1016/j.clinbiomech.2015.06.005.

[7] L.C. Schmitt, M. V. Paterno, T.E. Hewett, The Impact of Quadriceps Femoris Strength Asymmetry on Functional Performance at Return to Sport Following Anterior Cruciate Ligament Reconstruction, J. Orthop. Sport. Phys. Ther. 42 (2012) 750–759. doi:10.2519/jospt.2012.4194.

[8] C.A. Emery, Risk factors for injury in child and adolescent sport: A systematic review of the literature, Clin. J. Sport Med. 13 (2003) 256–268. doi:10.1097/00042752-200307000-00011.

[9] C.L. Ardern, N.F. Taylor, J.A. Feller, K.E. Webster, Fifty-five per cent return to competitive sport following anterior cruciate ligament reconstruction surgery : an updated systematic

review and meta-analysis including aspects of physical functioning and contextual factors, Br. J. Sports Med. 48 (2014) 1543–1552. doi:10.1136/bjsports-2013-093398.

[10] N.E. Van Melick, R.E.H. Van Cingel, T.G. Van Tienen, Functional performance 2-9 years after ACL reconstruction: cross-sectional comparison between athletes with bone-patellar tendon-bone, semitendinosus/gracilis and healthy controls, Knee Surgery, Sport. Traumatol. Arthrosc. 25 (2017) 1412–1423. doi:10.1007/s00167-015-3801-7.

[11] H. Grindem, L. Snyder-Mackler, H. Moksnes, L. Engebretsen, M.A. Risberg, SIMPLE DECISION RULES REDUCE REINJURY RISK AFTER ANTERIOR CRUCIATE LIGAMENT RECONSTRUCTION: THE DELAWARE-OSLO ACL COHORT STUDY, Br. J. Sports Med. 50 (2016) 804–808. doi:10.1136/bjsports-2016-096031.SIMPLE.

[12] R. Tyler Hamilton, S.J. Shultz, R.J. Schmitz, D.H. Perrin, Triple-Hop Distance as a Valid Predictor of Lower Limb Strength and Power, J. Athl. Train. 43 (2008) 144–151. doi:10.4085/1062-6050-43.2.144.

[13] G.K. Fitzgerald, S.M. Lephart, J.H. Hwang, M.R.S. Wainner, Hop Tests as Predictors of Dynamic Knee Stability, J. Orthop. Sport. Phys. Ther. 31 (2001) 588–597. doi:10.2519/jospt.2001.31.10.588.

[14] D. Logerstedt, H. Grindem, A. Lynch, I. Eitzen, L. Engebretsen, M.A. Risberg, M.J. Axe, L. Snyder-mackler, Single-Legged Hop Tests as Predictors of Self-Reported Knee Function After Anterior Cruciate Ligament Reconstruction, Am. J. Sports Med. 40 (2012) 2348–2356. doi:10.1177/0363546512457551.

[15] E. Rohman, J.T. Steubs, M. Tompkins, Changes in Involved and Uninvolved Limb Function During Rehabilitation After Anterior Cruciate Ligament Reconstruction: Implications for Limb Symmetry Index Measures, Am. J. Sports Med. 43 (2015) 1391–1398. doi:10.1177/0363546515576127.

[16] S.A. Xergia, E. Pappas, F. Zampeli, S. Georgiou, A.D. Georgoulis, Asymmetries in Functional Hop Tests, Lower Extremity Kinematics, and Isokinetic Strength Persist 6 to 9 Months Following Anterior Cruciate Ligament Reconstruction, J. Orthop. Sport. Phys. Ther. 43 (2013) 154–162. doi:10.2519/jospt.2013.3967.

[17] S.A. Xergia, E. Pappas, A.D. Georgoulis, Association of the Single-Limb Hop Test With Isokinetic, Kinematic, and Kinetic Asymmetries in Patients After Anterior Cruciate Ligament Reconstruction, Sports Health. 7 (2014) 217–223. doi:10.1177/1941738114529532.

[18] M. O'Reilly, B. Caulfield, T. Ward, W. Johnston, C. Doherty, Wearable Inertial Sensor Systems for Lower Limb Exercise Detection and Evaluation: A Systematic Review, Sport. Med. 48 (2018) 1221–1246. doi:10.1007/s40279-018-0878-4.

[19] T.A.L. Wren, N.M. Mueske, C.H. Brophy, J.L. Pace, M.J. Katzel, B.R. Edison, C.D. VandenBerg, T.L. Zaslow, Hop Distance Symmetry Does Not Indicate Normal Landing Biomechanics in Adolescent Athletes With Recent Anterior Cruciate Ligament Reconstruction, J. Orthop. Sport. Phys. Ther. (2018) 1–23. doi:10.2519/jospt.2018.7817.

[20] K.F. Orishimo, I.J. Kremenic, M.J. Mullaney, M.P. McHugh, S.J. Nicholas, Adaptations in single-leg hop biomechanics following anterior cruciate ligament reconstruction, Knee Surgery, Sport. Traumatol. Arthrosc. 18 (2010) 1587–1593. doi:10.1007/s00167-010-1185-2.

[21] A. Gokeler, A.L. Hof, M.P. Arnold, P.U. Dijkstra, K. Postema, E. Otten, Abnormal landing strategies after ACL reconstruction, Scand. J. Med. Sci. Sport. 20 (2010) 12–19. doi:10.1111/j.1600-0838.2008.00873.x.

[22] J. Favre, B.M. Jolles, R. Aissaoui, K. Aminian, Ambulatory measurement of 3D knee joint angle, J. Biomech. 41 (2008) 1029–1035. doi:10.1016/j.jbiomech.2007.12.003.

[23] H. Rouhani, J. Favre, X. Crevoisier, K. Aminian, Measurement of Multi-segment Foot Joint Angles During Gait Using a Wearable System, J. Biomech. Eng. 134 (2012) 061006. doi:10.1115/1.4006674.

[24] B. Mariani, C. Hoskovec, S. Rochat, C. Büla, J. Penders, K. Aminian, 3D gait assessment in young and elderly subjects using foot-worn inertial sensors, J. Biomech. 43 (2010) 2999–3006. doi:10.1016/j.jbiomech.2010.07.003.

[25] B. Mariani, H. Rouhani, X. Crevoisier, K. Aminian, Gait & Posture Quantitative estimation of foot-flat and stance phase of gait using foot-worn inertial sensors, Gait Posture. 37 (2013)

229–234. doi:10.1016/j.gaitpost.2012.07.012.

[26] A. Salarian, H. Russmann, F.J.G. Vingerhoets, C. Dehollain, Y. Blanc, P.R. Burkhard, K. Aminian, Gait assessment in Parkinson's disease: Toward an ambulatory system for long-term monitoring, IEEE Trans. Biomed. Eng. 51 (2004) 1434–1443. doi:10.1109/TBME.2004.827933.

[27] K. Aminian, B. Najafi, C. Büla, P.-F. Leyvraz, P. Robert, Spatio-temporal parameters of gait measured by an ambulatory system using miniature gyroscopes, J. Biomech. 35 (2002) 689–699. doi:10.1016/S0021-9290(02)00008-8.

[28] T. Seel, J. Raisch, T. Schauer, IMU-Based Joint Angle Measurement for Gait Analysis, Sensors. 14 (2014) 6891–6909. doi:10.3390/s140406891.

[29] A.M. Sabatini, C. Martelloni, S. Scapellato, F. Cavallo, Assessment of Walking Features From Foot Inertial Sensing, IEEE Trans. Biomed. Eng. 52 (2005) 486–494. doi:10.1016/j.sna.2005.03.052.

[30] A. V. Dowling, J. Favre, T.P. Andriacchi, A Wearable System to Assess Risk for Anterior Cruciate Ligament Injury During Jump Landing: Measurements of Temporal Events, Jump Height, and Sagittal Plane Kinematics, J. Biomech. Eng. 133 (2011) 071008. doi:10.1115/1.4004413.

[31] C. Jakob, P. Kugler, F. Hebenstreit, S. Reinfelder, U. Jensen, D. Schuldhaus, M. Lochmann, B. Eskofier, Estimation of the Knee Flexion-Extension Angle During Dynamic Sport Motions Using Body-worn Inertial Sensors, Proc. 8th Int. Conf. Body Area Networks. (2013) 289–295. doi:10.4108/icst.bodynets.2013.253613.

[32] L. Quagliarella, N. Sasanelli, G. Belgiovine, L. Moretti, Evaluation of standing vertical jump by ankles acceleration measurement, J. Strength Cond. Res. 24 (2010) 23–27.

[33] I. Setuain, M. González-Izal, J. Alfaro, E. Gorostiaga, M. Izquierdo, Acceleration and Orientation Jumping Performance Differences Among Elite Professional Male Handball Players With or Without Previous ACL Reconstruction: An Inertial Sensor Unit-Based Study, PM R. 7 (2015) 1243–1253. doi:10.1016/j.pmrj.2015.05.011.

[34] S. Zihajehzadeh, T.J. Lee, J.K. Lee, R. Hoskinson, E.J. Park, Integration of MEMS inertial

and pressure sensors for vertical trajectory determination, IEEE Trans. Instrum. Meas. 64 (2015) 804–814. doi:10.1109/TIM.2014.2359813.

[35] R. Petschnig, R. Baron, M. Albrecht, The Relationship Between Isokinetic Quadriceps Strength Test and Hop Tests for Distance and One-Legged Vertical Jump Test Following Anterior Cruciate Ligament Reconstruction, J. Orthop. Sport. Phys. Ther. 28 (1998) 23–31.

[36] L.A. Bolgla, D.R. Keskula, Reliability of Lower Extremity Functional Performance Tests, J. Orthop. Sport. Phys. Ther. 26 (1997) 138–142. doi:10.2519/jospt.1997.26.3.138.

[37] J. Augustsson, R. Thomeé, C. Lindén, M. Folkesson, R. Tranberg, J. Karlsson, Single-leg hop testing following fatiguing exercise: Reliability and biomechanical analysis, Scand. J. Med. Sci. Sport. 16 (2006) 111–120. doi:10.1111/j.1600-0838.2005.00446.x.

[38] P.T. Johnston, J.A. Mcclelland, K.E. Webster, Lower Limb Biomechanics During Single-Leg Landings Following Anterior Cruciate Ligament Reconstruction : A Systematic Review and Meta-Analysis, Sport. Med. (2018) 1–24. doi:10.1007/s40279-018-0942-0.

[39] S.D. Barber, F.R. Noyes, R.E. Mangine, J.W. McCloskey, W. Hartman, Quantitative assessment of functional limitations in normal and anterior cruciate ligament-deficient knees, Clin. Orthop. Relat. Res. (1990) 204–214. doi:10.1097/00003086-199006000-00028.

[40] K.F. Orishimo, I.J. Kremenic, Effect of fatigue on single-leg hop landing biomechanics, J. Appl. Biomech. 22 (2006) 245–254. doi:10.1123/jab.22.4.245.

[41] E.J. Hegedus, S. Mcdonough, C. Bleakley, C.E. Cook, G.D. Baxter, Clinician-friendly lower extremity physical performance measures in athletes: a systematic review of measurement properties and correlation with injury, part 1. The tests for knee function including the hop tests, Br. J. Sports Med. 49 (2015) 642–648. doi:10.1136/bjsports-2014-094094.

[42] E.M. Roos, H.P. Roos, L.S. Lohmander, C. Ekdahl, B.D. Beynnon, Knee Injury and Osteoarthritis Outcome Score (KOOS) - Development of a self-administered outcome measure, J. Orthop. Sports Phys. Ther. 28 (1998) 88–96. doi:10.2519/jospt.1998.28.2.88.

[43] N.J. Collins, C.A.C. Prinsen, R. Christensen, E.M. Bartels, C.B. Terwee, E.M. Roos, Knee

Injury and Osteoarthritis Outcome Score (KOOS): systematic review and meta-analysis of measurement properties, Osteoarthr. Cartil. 24 (2016) 1317–1329. doi:10.1016/j.joca.2016.03.010.

[44] M. Salavati, B. Akhbari, F. Mohammadi, M. Mazaheri, M. Khorrami, Knee injury and Osteoarthritis Outcome Score (KOOS); reliability and validity in competitive athletes after anterior cruciate ligament reconstruction, Osteoarthr. Cartil. 19 (2011) 406–410. doi:10.1016/j.joca.2011.01.010.

[45] J.J. van der Harst, A. Gokeler, A.L. Hof, Leg kinematics and kinetics in landing from a single-leg hop for distance. A comparison between dominant and non-dominant leg, Clin. Biomech. 22 (2007) 674–680. doi:10.1016/j.clinbiomech.2007.02.007.

[46] A. Kotsifaki, V. Korakakis, R. Whiteley, S. Van Rossom, I. Jonkers, Measuring only hop distance during single leg hop testing is insufficient to detect deficits in knee function after ACL reconstruction: A systematic review and meta-analysis, Br. J. Sports Med. (2019) 1–16. doi:10.1136/bjsports-2018-099918.

[47] A. Cappozzo, U. Della Croce, A. Leardini, L. Chiari, Human movement analysis using stereophotogrammetry. Part 1: Theoretical background, Gait Posture. 21 (2005) 186–196. doi:10.1016/j.gaitpost.2004.01.010.

[48] G. Wu, P.R. Cavanagh, ISB recommendations for standardization in the reporting of kinematic data, J. Biomech. 28 (1995) 1257–1261. doi:10.1016/0021-9290(95)00017-C.

[49] A. Cappozzo, F. Catan, U. Della Croce, A. Leardini, Cappozzo_CB_1995, Clin. Biomech. 10 (1995) 171–178. doi:10.1016/0268-0033(95)91394-T.

[50] E.S. Grood, W.J. Suntay, A joint coordinate system for the clinical description of three-dimensional motions: application to the knee, J. Biomech. Eng. 105 (1983) 136–144.

[51] G. Wu, S. Siegler, P. Allard, C. Kirtley, A. Leardini, D. Rosenbaum, M. Whittle, D. D D'Lima, L. Cristofolini, H. Witte, O. Schmid, ISB recommendation on definitions of joint coordinate system of various joints for the reporting of human joint motion-part I: ankle, hip, and spine, J. Biomech. 35 (2002) 543–548. doi:10.1188/02.onf.623.

[52] H.J. Woltring, Representation and calculation of 3-D joint movement, Hum. Mov. Sci. 10

(1991) 603–616. doi:10.1016/0167-9457(91)90048-3.

[53] J. Favre, Ambulatory Evaluation of 3D Knee Joint Function in Patients with ACL Rupture Using Inertial Sensors, 2008.

[54] B. Fasel, J. Spörri, J. Chardonnens, J. Kröll, E. Müller, K. Aminian, Joint Inertial Sensor Orientation Drift Reduction for Highly Dynamic Movements, IEEE J. Biomed. Heal. INFORMATICS. 22 (2018) 77–86.

[55] B. Fasel, J. Spörri, P. Schütz, S. Lorenzetti, K. Aminian, Validation of functional calibration and strap-down joint drift correction for computing 3D joint angles of knee, hip, and trunk in alpine skiing, PLoS One. 12 (2017) 1–18. doi:10.1371/journal.pone.0181446.

[56] H. Dejnabadi, B.M. Jolles, E. Casanova, P. Fua, K. Aminian, Estimation and visualization of sagittal kinematics of lower limbs orientation using body-fixed sensors, IEEE Trans. Biomed. Eng. 53 (2006) 1385–1393. doi:10.1109/TBME.2006.873678.

[57] H. Dejnabadi, B.M. Jolles, K. Aminian, A new approach to accurate measurement of uniaxial joint angles based on a combination of accelerometers and gyroscopes, IEEE Trans. Biomed. Eng. 52 (2005) 1478–1484. doi:10.1109/TBME.2005.851475.

[58] M. Nazarahari, A. Noamani, N. Ahmadian, H. Rouhani, Sensor-to-body calibration procedure for clinical motion analysis of lower limb using magnetic and inertial measurement units, J. Biomech. (2019) 1–6. doi:10.1016/j.jbiomech.2019.01.027.

[59] J. Favre, R. Aissaoui, B.M. Jolles, J.A. de Guise, K. Aminian, Functional calibration procedure for 3D knee joint angle description using inertial sensors, J. Biomech. 42 (2009) 2330–2335. doi:10.1016/j.jbiomech.2009.06.025.

[60] E. Palermo, S. Rossi, F. Marini, F. Patanè, P. Cappa, Experimental evaluation of accuracy and repeatability of a novel body-to-sensor calibration procedure for inertial sensor-based gait analysis, Meas. J. Int. Meas. Confed. 52 (2014) 145–155. doi:10.1016/j.measurement.2014.03.004.

[61] R.W. Selles, M.A.G. Formanoy, J.B.J. Bussmann, P.J. Janssens, H.J. Stam, Automated estimation of initial and terminal contact timing using accelerometers; development and validation in transtibial amputees and controls, IEEE Trans. Neural Syst. Rehabil. Eng. 13

(2005) 81–88. doi:10.1109/TNSRE.2004.843176.

[62] A.M. Sabatini, Quaternion-based strap-down integration method for applications of inertial sensing to gait analysis, Med. Biol. Eng. Comput. 43 (2005) 94–101.

[63] A. Peruzzi, U. Della Croce, A. Cereatti, Estimation of stride length in level walking using an inertial measurement unit attached to the foot : A validation of the zero velocity assumption during stance, J. Biomech. 44 (2011) 1991–1994. doi:10.1016/j.jbiomech.2011.04.035.

[64] E. Poulsen, G.H. Goncalves, A. Bricca, E.M. Roos, J.B. Thorlund, C.B. Juhl, Knee osteoarthritis risk is increased 4-6 fold after knee injury – a systematic review and meta-analysis, Br. J. Sports Med. (2019) 1–11. doi:10.1136/bjsports-2018-100022.

[65] T.P. Andriacchi, A. Mündermann, R.L. Smith, E.J. Alexander, C.O. Dyrby, S. Koo, A Framework for the in Vivo Pathomechanics of Osteoarthritis at the Knee, Ann. Biomed. Eng. 32 (2004) 447–457.

[66] V. Silverwood, M. Blagojevic-Bucknall, C. Jinks, J.. Jordan, J. Protheroe, K.. Jordan, Current evidence on risk factors for knee osteoarthritis in older adults: a systematic review and meta-analysis, Osteoarthr. Cartil. 23 (2015) 507–515. doi:10.1016/j.joca.2014.11.019.

[67] P.E. Roos, K. Button, V. Sparkes, R.W.M. van Deursen, Altered biomechanical strategies and medio-lateral control of the knee represent incomplete recovery of individuals with injury during single leg hop, J. Biomech. 47 (2014) 675–680. doi:10.1016/j.jbiomech.2013.11.046.

[68] H. Grindem, D. Logerstedt, I. Eitzen, H. Moksnes, M.J. Axe, L. Snyder-Mackler, L. Engebretsen, M.A. Risberg, Single-legged Hop tests as predictors of self-reported knee function in nonoperatively treated individuals with anterior cruciate ligament injury, Am. J. Sports Med. 39 (2011) 2347–2354. doi:10.1177/0363546511417085.

[69] I. Holm, A.T. Tveter, P.M. Fredriksen, N. Vøllestad, A normative sample of gait and hopping on one leg parameters in children 7-12 years of age, Gait Posture. 29 (2009) 317–321. doi:10.1016/j.gaitpost.2008.09.016.

[70] K. Button, P.E. Roos, R.W.M. Van Deursen, Activity progression for anterior cruciate

ligament injured individuals, Clin. Biomech. 29 (2014) 206–212. doi:10.1016/j.clinbiomech.2013.11.010.

[71] E. Wellsandt, E.S. Gardinier, K. Manal, M.J. Axe, T.S. Buchanan, L. Snyder-Mackler, Decreased Knee Joint Loading Associated With Early Knee Osteoarthritis After Anterior Cruciate Ligament Injury, Am. J. Sports Med. 44 (2016) 143–151. doi:10.1007/BF00612995.

[72] M. Boutaayamou, C. Schwartz, J. Stamatakis, V. Denoël, D. Maquet, B. Forthomme, J. Croisier, B. Macq, J.G. Verly, G. Garraux, O. Brüls, Development and validation of an accelerometer-based method for quantifying gait events, Med. Eng. Phys. J. 37 (2015) 226–232. doi:10.1016/j.medengphy.2015.01.001.

[73] E.M. Roos, L.S. Lohmander, Health and Quality of Life Outcomes The Knee injury and Osteoarthritis Outcome Score (KOOS): from joint injury to osteoarthritis The Knee injury and Osteoarthritis Outcome Score (KOOS), Health Qual. Life Outcomes. 1 (2003) 1–8. https://hqlo.biomedcentral.com/track/pdf/10.1186/1477-7525-1-64?site=hqlo.biomedcentral.com.

[74] J.L. Whittaker, L.J. Woodhouse, A. Nettel-aguirre, C.A. Emery, Outcomes associated with early post-traumatic osteoarthritis and other negative health consequences 3 e 10 years following knee joint injury in youth sport, Osteoarthr. Cartil. 23 (2015) 1122–1129. doi:10.1016/j.joca.2015.02.021.

[75] E. Roos, KOOS Knee Survey, KOOS Web Manag. (2012). www.koos.nu (accessed November 16, 2019).

Appendix A – Knee Injury and Osteoarthritis Outcome Score (KOOS) Questionnaire

The English version (LK1.0) of the KOOS questionnaire has been adopted from the KOOS website [75] for further insight into subscales that this questionnaire measures. Slight formatting, such as minor modifications in fonts, has been performed for consistency of the entire thesis.

KOOS KNEE SURVEY

Today's date: _____/_____/_____ Date of birth: _____/_____/_____

Name: _____

INSTRUCTIONS: This survey asks for your view about your knee. This information will help us keep track of how you feel about your knee and how well you are able to perform your usual activities.

Answer every question by ticking the appropriate box, only one box for each question. If you are unsure about how to answer a question, please give the best answer you can.

Symptoms

These questions should be answered thinking of your knee symptoms during the **last week**.

S1. Do you have swelling in your knee?

Never	Rarely	Sometimes	Often	Always
□	□	□	□	□

S2. Do you feel grinding, hear clicking or any other type of noise when your knee moves?

Never	Rarely	Sometimes	Often	Always
□	□	□	□	□

S3. Does your knee catch or hang up when moving?

Never	Rarely	Sometimes	Often	Always
□	□	□	□	□

S4. Can you straighten your knee fully?

Always	Often	Sometimes	Rarely	Never
□	□	□	□	□

S5. Can you bend your knee fully?

Always	Often	Sometimes	Rarely	Never
□	□	□	□	□

Stiffness

The following questions concern the amount of joint stiffness you have experienced during the **last week** in your knee. Stiffness is a sensation of restriction or slowness in the ease with which you move your knee joint.

S6. How severe is your knee joint stiffness after first wakening in the morning?

None	Mild	Moderate	Severe	Extreme
□	□	□	□	□

S7. How severe is your knee stiffness after sitting, lying or resting later in the day?

None	Mild	Moderate	Severe	Extreme
□	□	□	□	□

Pain

P1. How often do you experience knee pain?

Never	Monthly	Weekly	Daily	Always
□	□	□	□	□

What amount of knee pain have you experienced the **last week** during the following activities?

P2. Twisting/pivoting on your knee

None	Mild	Moderate	Severe	Extreme
□	□	□	□	□

P3. Straightening knee fully

None	Mild	Moderate	Severe	Extreme
□	□	□	□	□

P4. Bending knee fully

None	Mild	Moderate	Severe	Extreme
□	□	□	□	□

P5. Walking on flat surface

None	Mild	Moderate	Severe	Extreme
□	□	□	□	□

P6. Going up or down stairs

None	Mild	Moderate	Severe	Extreme
□	□	□	□	□

P7. At night while in bed

None	Mild	Moderate	Severe	Extreme
□	□	□	□	□

P8. Sitting or lying

None	Mild	Moderate	Severe	Extreme
□	□	□	□	□

P9. Standing upright

None	Mild	Moderate	Severe	Extreme
□	□	□	□	□

Function, daily living

The following questions concern your physical function. By this we mean your ability to move around and to look after yourself. For each of the following activities please indicate the degree of difficulty you have experienced in the **last week** due to your knee.

A1. Descending stairs

None	Mild	Moderate	Severe	Extreme
□	□	□	□	□

A2. Ascending stairs

None	Mild	Moderate	Severe	Extreme
□	□	□	□	□

For each of the following activities please indicate the degree of difficulty you have experienced in the **last week** due to your knee.

A3. Rising from sitting

None	Mild	Moderate	Severe	Extreme
□	□	□	□	□

A4. Standing

None	Mild	Moderate	Severe	Extreme
□	□	□	□	□

A5. Bending to floor/pick up an object

None	Mild	Moderate	Severe	Extreme
□	□	□	□	□

A6. Walking on flat surface

None	Mild	Moderate	Severe	Extreme
□	□	□	□	□

A7. Getting in/out of car

None	Mild	Moderate	Severe	Extreme
□	□	□	□	□

A8. Going shopping

None	Mild	Moderate	Severe	Extreme
□	□	□	□	□

A9. Putting on socks/stockings

None	Mild	Moderate	Severe	Extreme
□	□	□	□	□

A10. Rising from bed

None	Mild	Moderate	Severe	Extreme
□	□	□	□	□

A11. Taking off socks/stockings

None	Mild	Moderate	Severe	Extreme
□	□	□	□	□

A12. Lying in bed (turning over, maintaining knee position)

None	Mild	Moderate	Severe	Extreme
□	□	□	□	□

A13. Getting in/out of bath

None	Mild	Moderate	Severe	Extreme
□	□	□	□	□

A14. Sitting

None	Mild	Moderate	Severe	Extreme
□	□	□	□	□

A15. Getting on/off toilet

None	Mild	Moderate	Severe	Extreme
□	□	□	□	□

For each of the following activities please indicate the degree of difficulty you have experienced in the **last week** due to your knee.

A16. Heavy domestic duties (moving heavy boxes, scrubbing floors, etc.)

None	Mild	Moderate	Severe	Extreme
□	□	□	□	□

A17. Light domestic duties (cooking, dusting, etc.)

None	Mild	Moderate	Severe	Extreme
□	□	□	□	□

Function, sports and recreational activities

The following questions concern your physical function when being active on a higher level. The questions should be answered thinking of what degree of difficulty you have experienced during the **last week** due to your knee.

SP1. Squatting

None	Mild	Moderate	Severe	Extreme
□	□	□	□	□

SP2. Running

None	Mild	Moderate	Severe	Extreme
□	□	□	□	□

SP3. Jumping

None	Mild	Moderate	Severe	Extreme
□	□	□	□	□

SP4. Twisting/pivoting on your injured knee

None	Mild	Moderate	Severe	Extreme
□	□	□	□	□

SP5. Kneeling

None	Mild	Moderate	Severe	Extreme
□	□	□	□	□

Quality of Life

Q1. How often are you aware of your knee problem?

Never	Monthly	Weekly	Daily	Constantly
□	□	□	□	□

Q2. Have you modified your life style to avoid potentially damaging activities to your knee?

Not at all	Mildly	Moderately	Severely	Totally
□	□	□	□	□

Q3. How much are you troubled with lack of confidence in your knee?

Not at all	Mildly	Moderately	Severely	Extremely
□	□	□	□	□

Q4. In general, how much difficulty do you have with your knee?

None	Mild	Moderate	Severe	Extreme
□	□	□	□	□

Thank you very much for completing all the questions in this questionnaire.

Appendix B – Joints ROM Comparisons (*p*-Value Tables)

As described in Chapter 3, the knee and ankle ranges of motion (ROMs) in the sagittal plane and the limb symmetry indices (LSIs) of these kinematic parameters were compared between groups of injured and uninjured youth in Clinical Research Application Study (See Table 3 and Table 4). Table B-1 and Table B-2 indicate the *p*-values of these comparisons for inter-participant (between groups) and intra-participant (side-to-side) assessments, respectively.

Table B-1. *p*-values obtained from inter-participant comparisons (between groups comparisons) in Clinical Research Application study. Knee and ankle ranges of motion (ROMs) in the sagittal plane and their corresponding limb symmetry indices (LSIs) during all the hop phases are compared between groups of injured (G_I) and uninjured (G_{UI}) participants. Significant differences ($p<0.05$) are marked with asterisks and bold numbers.

Specification	Phase	Compared Leg Groups or Limb Symmetry Indices (LSIs)						
		G_I-I			G_I-NI			G_I LSI
		G_{UI}-B	G_{UI}-D	G_{UI}-ND	G_{UI}-B	G_{UI}-D	G_{UI}-ND	G_{UI} LSI
Ankle ROM	**Fly 1**	0.734	0.583	1.000	0.990	0.887	0.855	0.611
	Land 1	0.195	0.138	0.556	**0.048***	**0.030***	0.319	0.382
	Fly 2	0.678	0.281	0.699	0.232	0.186	0.556	0.100
	Land 2	0.428	0.730	0.360	0.345	0.556	0.360	0.452
	Fly 3	0.659	0.823	0.339	0.068	0.319	0.054	0.583
Knee ROM	**Fly 1**	0.811	0.452	0.730	0.772	0.529	0.887	0.149
	Land 1	0.678	0.730	0.300	0.242	0.951	0.070	0.215
	Fly 2	0.252	0.477	0.264	0.870	0.699	0.919	0.070
	Land 2	0.623	0.319	0.855	0.990	0.452	0.477	0.611
	Fly 3	**0.009***	0.118	**0.008***	0.085	0.529	**0.033***	**0.017***

Leg groups are shown with G_I-I: G_I's Injured Leg, G_I-NI: G_I's Non-Injured Leg, G_{UI}-D: G_{UI}'s Dominant Leg, G_{UI}-ND: G_{UI}'s Non-Dominant Leg and G_{UI}-B: G_{UI}'s Both Legs.

LSIs (in percentage) were calculated as the ratio of knee and ankle ROMs of injured (or non-dominant) leg of the participant over their non-injured (or dominant) knee and ankle ROMs.

Table B-2. *p*-values obtained from intra-participant comparisons (side-to-side comparisons) in Clinical Research Application study. Knee and ankle ranges of motion (ROMs) in the sagittal plane are compared side-to-side during all hop phases for groups of injured (G_I) and uninjured (G_{UI}) participants. Significant differences ($p<0.05$) are marked with asterisks and bold numbers.

Specification	Phase	Compared Leg Groups	
		Side-to-Side Comparison between G_{UI}-D and G_{UI}-ND	**Side-to-Side Comparison between G_I-I and G_I-NI**
Ankle ROM	**Fly 1**	0.432	0.158
	Land 1	0.432	0.733
	Fly 2	0.492	0.101
	Land 2	0.322	0.615
	Fly 3	**0.020***	**0.008***
Knee ROM	**Fly 1**	0.160	0.527
	Land 1	**0.020***	0.408
	Fly 2	0.375	0.200
	Land 2	**0.049***	0.236
	Fly 3	**0.010***	0.189

Leg groups are shown with G_I-I: G_I's Injured Leg, G_I-NI: G_I's Non-Injured Leg, G_{UI}-D: G_{UI}'s Dominant Leg, and G_{UI}-ND: G_{UI}'s Non-Dominant Leg.

Appendix C – Temporospatial Comparisons (*p*-Value Tables)

As described in Chapter 4, individual hop distances, total TSLH progression (measured with IMUs and a measuring tape), flying/landing times, and limb symmetry indices (LSIs) of these temporospatial parameters were compared between groups of injured and uninjured youth in Clinical Research Application Study (See Fig. 11). Table C-1 and Table C-2 indicate the *p*-values of these comparisons for inter-participant (between groups) and intra-participant (side-to-side) assessments, respectively.

Table C-1. *p*-values obtained from inter-participant comparisons (between groups comparisons) in Clinical Research Application study. Flying/landing times, hop distances (individual distances, and total TSLH progression measured with IMUs and a tape), and their corresponding limb symmetry indices (LSIs) are compared between groups of injured (G_I) and uninjured (G_{UI}) participants. A significant difference ($p<0.05$) is marked with an asterisk and a bold number.

Specification	Phase	Compared Leg Groups or Limb Symmetry Indices (LSIs)						
		G_I-I			G_I-NI			G_I LSI
		G_{UI}-B	G_{UI}-D	G_{UI}-ND	G_{UI}-B	G_{UI}-D	G_{UI}-ND	G_{UI} LSI
Flying/Landing Time	Fly 1	0.880	0.714	0.528	0.910	0.669	0.823	0.319
	Land 1	0.158	0.207	0.319	**0.049***	0.084	0.155	0.640
	Fly 2	0.141	0.215	0.263	0.920	0.903	0.984	0.161
	Land 2	0.051	0.070	0.186	0.241	0.167	0.626	0.887
	Fly 3	0.546	0.300	0.968	0.990	0.515	0.542	0.319
Hop Distance	Hop 1	0.641	0.699	0.730	0.970	1.000	0.951	0.556
	Hop 2	0.791	0.792	0.887	0.505	0.502	0.699	0.477
	Hop 3	0.678	0.792	0.699	0.320	0.428	0.428	0.230
	TSLH Total (IMUs)	0.850	0.760	1.000	0.641	0.699	0.730	0.360
	TSLH Total (Tape)	0.910	0.792	0.951	0.529	0.714	0.529	0.382

Leg groups are shown with G_I-I: G_I's Injured Leg, G_I-NI: G_I's Non-Injured Leg, G_{UI}-D: G_{UI}'s Dominant Leg, G_{UI}-ND: G_{UI}'s Non-Dominant Leg and G_{UI}-B: G_{UI}'s Both Legs.

Distance-based LSIs (in percentage) were calculated as the ratio of distance that participants have hopped with their injured leg over the distance they have achieved with their non-injured leg.

Time-based LSIs (in percentage) were calculated for each hop phase as the ratio of the time that the participants needed to hop on their non-injured leg over the time that they needed to hop on their injured leg.

Table C-2. *p*-values obtained from intra-participant comparisons (side-to-side comparisons) in Clinical Research Application study. Flying/landing times, and hop distances (individual distances, and total TSLH progression measured with IMUs and tape) are compared side-to-side for groups of injured (G_I) and uninjured (G_{UI}) participants. A significant difference ($p<0.05$) is marked with an asterisk and a bold number.

Specification	Phase	Compared Leg Groups	
		Side-to-Side Comparison between G_{UI}-D and G_{UI}-ND	**Side-to-Side Comparison between G_I-I and G_I-NI**
Flying/Landing Time	**Fly 1**	0.359	0.681
	Land 1	0.770	0.858
	Fly 2	0.791	0.115
	Land 2	0.574	0.436
	Fly 3	0.111	0.741
Hop Distance	**Hop 1**	0.846	0.307
	Hop 2	0.492	0.910
	Hop 3	0.770	0.072
	TSLH Total (IMUs)	0.625	0.088
	TSLH Total (Tape)	0.154	**0.028***

Leg groups are shown with G_I-I: G_I's Injured Leg, G_I-NI: G_I's Non-Injured Leg, G_{UI}-D: G_{UI}'s Dominant Leg, and G_{UI}-ND: G_{UI}'s Non-Dominant Leg.

Appendix D – Other Relevant Signal Features for TSLH Temporal Events Detection

As described within the body of this thesis, all kinematic signal features proposed by Aminian [27], Salarian [26], Selles [61], and Mariani [25] for gait, were adapted for TSLH and implemented for both foot and shank IMUs. Table D-1 and Table D-2 show the errors of initial contact (IC) and terminal contact (TC) instants detection based on these kinematic features. According to these tables, features M12-IC, M11-IC, M8-IC, M4-IC, and M1-IC are the best representatives of IC instant, while M6-TC, M7-TC, and M1-TC are the best representatives of TC instant.

Table D-1. Errors of the proposed kinematic signal features in the estimation of IC instants of TSLH against the motion-capture system. Results are expressed as 25%, 50% and 75% percentiles of error, calculated for all 60 individual hops (20 TSLH trials, 3 hops each) performed by the 10 able-bodied participants.

IC Detection Method	Sensor Position	Feature	Signal	Rule	Error (ms)			Absolute Error (ms)		
					[0.25	0.5	0.75]	[0.25	0.5	0.75]
Salarian	Shank	S – IC	Ω_p	Min	[-9	12	40]	[10	26	40]
Aminian	Shank	A – IC	Wavelet of Ω_p	Min	[-6	15	36]	[9	22	36]
Mariani	Foot	M1 – IC	Ω_p	Min	[-15	6	16]	[7	16	31]
Mariani	Foot	M2 – IC	Ω_p	First Min	[4	16	49]	[12	24	49]
Mariani	Foot	M3 – IC	Ω_p	Zero Crossing	[32	62	81]	[32	62	81]
Mariani	Foot	M4 – IC	$\|\|A\|\|$	Min	[0	6	18]	[5	12	24]
Mariani	Foot	M5 – IC	$\|\|A\|\|$	Max	[-18	-7	2]	[6	9	18]
Mariani	Shank	M6 – IC	Ω_p	First Min	[-9	12	38]	[10	24	40]
Mariani	Shank	M7 – IC	Ω_p	First Max[(a)]	[-18	4	22]	[10	18	36]
Mariani	Shank	M8 – IC	Ω_p	First Max[(b)]	[-18	-4	11]	[7	16	23]
Mariani	Shank	M9 - IC	Ω_p	Zero Crossing	[10	42	63]	[18	42	63]
Mariani	Shank	M10 - IC	$\|\|A\|\|$	Max	[-43	-24	-11]	[12	24	43]
Mariani	Shank	M11 - IC	$\|(\|\|A\|\|')\|$	Max[(c)]	[-7	4	14]	[4	13	22]
Mariani	Shank	M12 - IC	$\|(\|\|A\|\|')\|$	Max[(d)]	[-9	2	12]	[4	12	20]

[(a)] First Maximum after M6 - IC
[(b)] First Maximum after M6 - IC (Peak Prominence > 0.05 rad)
[(c)] First Maximum (Peak Height > 5 m/s^3)
[(d)] First Maximum (Peak Height > 7 m/s^3)

Table D-2. Errors of the proposed kinematic signal features in the estimation of TC instants of TSLH against the motion-capture system. Results are expressed as 25%, 50% and 75% percentiles of error, calculated for all 60 individual hops (20 TSLH trials, 3 hops each) performed by the 10 able-bodied participants.

TC Detection Method	Sensor Position	Feature	Signal	Rule	Error (ms)			Absolute Error (ms)		
					[0.25	**0.5**	**0.75]**	**[0.25**	**0.5**	**0.75]**
Salarian	Shank	S - TC	Ω_p	Min	[-60	-37	-22]	[22	37	60]
Aminian	Shank	A - TC	Ω_p	Min	[-48	-26	-8]	[12	29	49]
Selles	Shank	SE - TC	A_v & A_F	Min	[-24	-8	17]	[9	21	30]
Mariani	Foot	M1 - TC	Ω_p	Min	[-1	15	20]	[10	18	27]
Mariani	Foot	M2 - TC	Ω_p	Zero Crossing	[-63	-37	-17]	[17	37	63]
Mariani	Foot	M3 - TC	$\|\|A\|\|$	Max	[-38	-9	4]	[6	14	38]
Mariani	Foot	M4 - TC	$\|\|\Omega\|\|'$	Min	[-30	-8	9]	[8	14	30]
Mariani	Foot	M5 - TC	$\|\|\Omega\|\|'$	Max	[8	27	47]	[14	32	48]
Mariani	Foot	M6 - TC	$\|\|\Omega\|\|'$	Value Crossing[(a)]	[-7	11	16]	[10	14	20]
Mariani	Foot	M7 - TC	$\|\|\Omega\|\|'$	Value Crossing[(b)]	[-5	12	18]	[10	14	20]
Mariani	Foot	M8 - TC	$\|(\|\|A\|\|')\|$	Max	[-28	-2	9]	[7	14	33]
Mariani	Shank	M9 - TC	$\|\|A\|\|$	Max	[-19	16	30]	[18	26	53]
Mariani	Shank	M10 - TC	$\|\Omega_p\|$	Max	[-47	-20	-1]	[10	21	47]

[(a)] First Point Below -0.6 rad/s^2

[(b)] First Point Below -0.5 rad/s^2

In these tables Ω_p, and $||\Omega||$ denote pitch angular velocity and norm of angular velocity, and A_v, A_F, and $||A||$ denote vertical acceleration, frontal acceleration, and norm of acceleration, respectively.